Inorganic Chemistry
Cite This: Inorg. Chem. XXXX, XXX, XXX−XXX
Article
pubs.acs.org/IC

Cobalt(I) Complexes of 5-Aryl-2-iminopyrrolyl Ligands: Synthesis, Spin Isomerism, and Application in Catalytic Hydroboration

Tiago F. C. Cruz, Luís F. Veiros, and Pedro T. Gomes*

Centro de Química Estrutural, Departamento de Engenharia Química, Instituto Superior Técnico, Universidade de Lisboa, Av. Rovisco Pais 1, 1049-001 Lisboa, Portugal

Supporting Information

ABSTRACT: This work reports the first successful isolation and full characterization of cobalt(I) complexes of 5-aryl-2-iminopyrrolyl ligands. In one approach, when [Co{κ^2*N*,*N*′-5-(2,4,6-R_3-C_6H_2)-NC_4H_2-2-C(H)=N(2,6-^{i}Pr$_2$-C_6H_3)}(Py)Cl] (R = ^{i}Pr, **1a**; R = Ph, **1b**) were reacted with K(HBEt$_3$) or Na(Hg) in toluene, the Co(I) arene complexes [Co{κ^2*N*,*N*′-5-(2,4,6-^{i}Pr$_3$-C_6H_2)-NC_4H_2-2-C(H)=N(2,6-^{i}Pr$_2$-C_6H_3)}(η^6-$C_6H_5CH_3$)] (**2a**) and [Co{κ^2*N*,*N*′-5-[2′-(κ:η^6-C_6H_5)-C_6H_2-4′,6′-Ph_2]-NC_4H_2-2-C(H)=N(2,6-^{i}Pr$_2$-C_6H_3)}] (**2b**) were formed. The reaction of complex **1a** with KC_8 in Et_2O yielded the [Co{κ^2*N*,*N*′-5-(2,4,6-^{i}Pr$_3$-C_6H_2)-NC_4H_2-2-C(H)=N(2,6-^{i}Pr$_2$-C_6H_3)}]$_2$ (**3**). On another approach, the metathesis of potassium 5-(2,4,6-triisopropylphenyl)-2-(*N*-2,6-diisopropylphenylformimino)-pyrrolyl (**KLa**) with CoCl(PMe$_3$)$_3$ yielded the bis(trimethylphosphine) complex [Co{κ^2*N*,*N*′-5-(2,4,6-^{i}Pr$_3$-C_6H_2)-NC_4H_2-2-C(H)=N(2,6-^{i}Pr$_2$-C_6H_3)}(PMe$_3$)$_2$] (**4**) in a good yield. Complexes **2a**, **3**, and **4** are paramagnetic, high-spin species, while **2b** is a diamagnetic complex. Compound **2b** exhibited a spin isomerism behavior ($S = 0 \leftrightarrow S = 1$) as determined by variable-temperature ^{1}H NMR experiments (ΔH° = 7.7 kcal mol^{-1}), being also supported by computational studies (ΔE = 4.2 kcal mol^{-1}). All complexes were tested in the hydroboration of styrene with pinacolborane (HBPin), with complex **4** exclusively yielding the respective anti-Markovnikov addition product. Additionally, all complexes catalyzed the fast and quantitative hydroboration of benzaldehyde with HBPin.

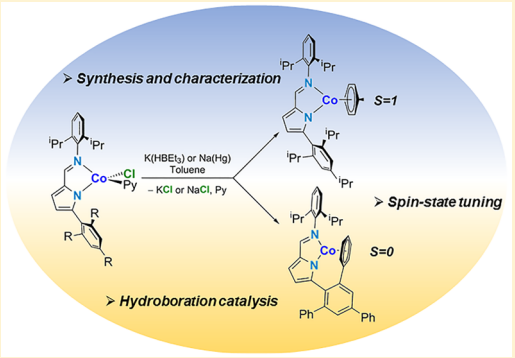

INTRODUCTION

The isolation of transition-metal complexes in low oxidation state and low coordination number has been pivotal in diverse fields, from small molecule activation and biomimetics[1] to catalysis involving the activation of hydrocarbons or ketones.[2] Many advances in the isolation of transition-metal complexes in low oxidation states with bidentate chelating ligands have been made, most notably with the β-diketiminate framework.[3]

Specifically considering Co complexes in low oxidation states with bidentate chelating ligands, some remarkable results are to be noted on the way to their isolation. One case, reported by Holland et al., is the binding of dinitrogen yielding the complexes [LCoN_2CoL] or [M_2{LCoN_2CoL}], with L being a bulky β-diketiminate bidentate ligand and M = Na, K (Chart 1, **A**).[4] Another interesting result is the formation of a Co−Co interaction in the complex [Co_2L_2], (with L being amidinate or guanidinate bidentate ligands (R = ^{t}Bu, N(^{i}Pr)$_2$, or N(Cy)$_2$; Chart 1, **B**), reported by Jones and co-workers.[5] Other notable results obtained when isolating low-valent Co complexes have resulted from noninnocent behavior of the supporting chelating ligand. For example, a coordination of an aryl ring of a chelating imine in a [LCo]$_2$ arrangement, with L being an α-diiminate ligand (derived from *N*,*N*′-bis(2,6-diisopropylphenyl)-2,3-dimethyl-1,4-diazabuta-1,3-diene)[6] (Chart 1, **C**) or a bulky β-diketiminate bidentate ligand[7] (Chart 1, **D**) have been observed. Interestingly, an LCo(THF) complex, with L being a bulky β-diketiminate chelate and THF being tetrahydrofuran, undergoes an isomerization process ending up in an unusual slipped $\kappa N,\eta^6$-arene binding mode in the resulting new LCo complex (Chart 1, **E**).[8] A redox noninnocence was also verified when isolating the Co(0) complex LCo(COD), with L being an α-diiminate ligand (derived from 1,2-bis(2,6-diisopropylphenylimino)acenaphthene (BIAN)) and COD = 1,5-cyclooctadiene (Chart 1, **F**), with applications in P_4 activations.[9]

The synthesis of low-valent Co complexes has recently paved the way to well-defined catalytic systems. For instance, owing to the importance of boronate esters in organic synthesis, late transition-metal complexes have been increasingly used in catalytic systems for the hydroboration of alkenes[10] and, sparsely, of aldehydes[11] and ketones.[12] In an example of a well-defined Co(I) catalyst in alkene hydroboration, Chirik and co-workers reported good yields of the respective organoborane reaction products with anti-Markovnikov selectivity, under neat and mild conditions, using a tridentate (bis(arylimino)pyridine)CoMe complex.[10b]

The great majority of first-row transition-metal complexes bearing 2-iminopyrrolyl ligands involve the coordination of

Received: August 23, 2018

DOI: 10.1021/acs.inorgchem.8b02392
Inorg. Chem. XXXX, XXX, XXX−XXX

Chart 1. Examples of Low-Valent Co Complexes (A–F) Containing Monoanionic Bidentate Chelates

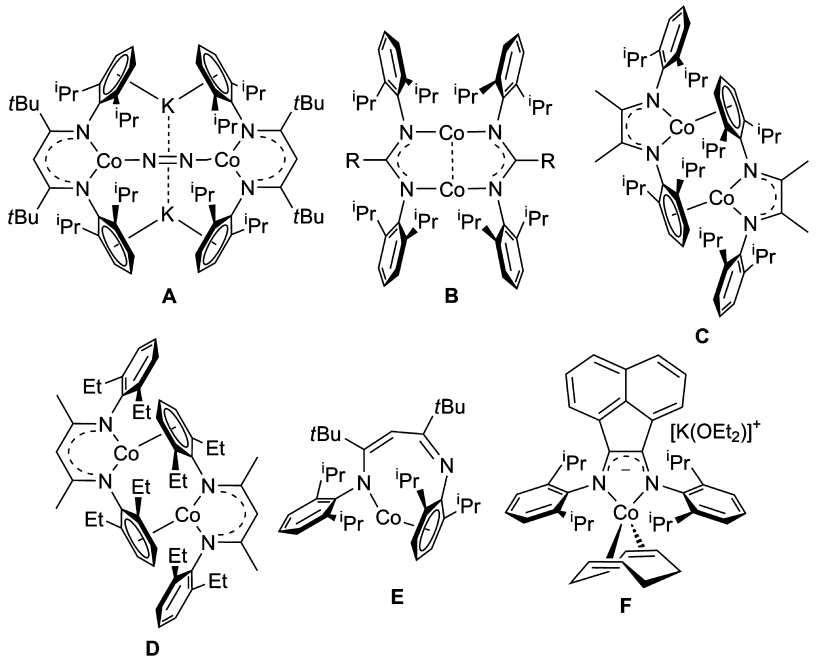

two of these ligands. Many complexes of the type [M(2-iminopyrrolyl)$_2$],[13] including some made in our group,[14] have been reported (Chart 2, **A**). To avoid the bis-homoleptic coordination

Chart 2. Homoleptic (A) and Heteroleptic Co(II) (B) 2-Iminopyrrolyl Complexes

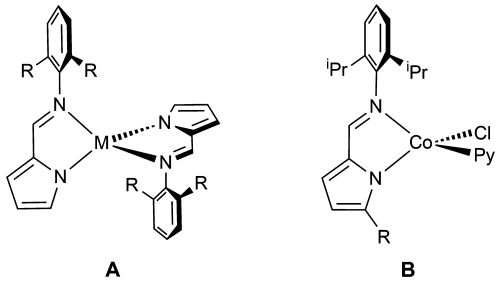

chemistry thermodynamic sink, we recently reported the preparation of bulky 5-aryl-2-iminopyrrole ligand precursors. These compounds allowed the preparation of Co(II)[15] complexes (Chart 2, **B**) of a single chelating 5-substituted-2-iminopyrrolyl ligand, which were also prepared in our group, having proved to be active in the hydroboration of terminal α-olefins, upon activation by K(HBEt$_3$).

The latter Co(II) complexes served as the starting point for the present study. Initially, the goal of this work was the understanding of the activation mode of these complexes (Chart 2, **B**) with K(HBEt$_3$) in the hydroboration of terminal α-olefins, which culminated in the synthesis and characterization of the first examples of Co(I) complexes bearing a 5-aryl-2-iminopyrrolyl ligand. The present study also addresses the high dependence of their electronic structures on the nature of the 5-aryl substituents employed and their behavior as efficient well-defined catalysts for the hydroboration of terminal alkenes and arylaldehydes with pinacolborane.

RESULTS AND DISCUSSION

Synthesis and Characterization of Co(I) Complexes Stabilized by Arene Ligands. To understand the mode of activation of the pyridine chloride Co(II) complexes with super hydrides,[15] we attempted some stochiometric reactions with K(HBEt$_3$) in toluene (Scheme 1, route a). On the one hand,

Scheme 1. Synthesis of Complexes 2a and 2b from 1a and 1b, Respectively[a]

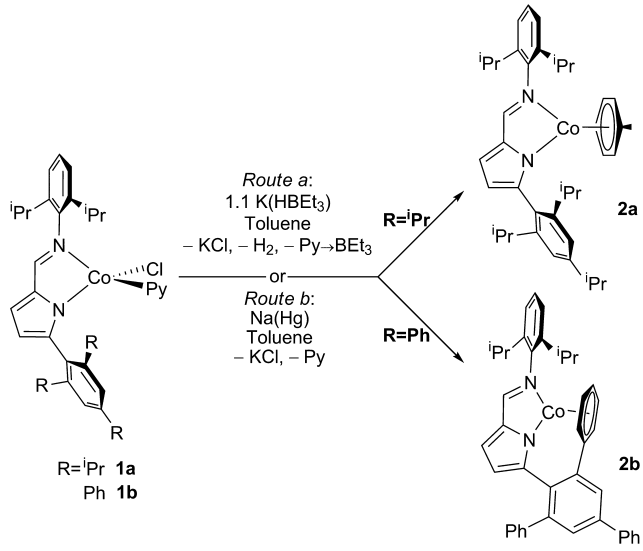

[a]Route a: Reactions of **1a** and **1b** with K(HBEt$_3$) in toluene. Route b: Reactions of **1a** and **1b** with Na(Hg), in toluene.

the reaction of a dark blue-violet toluene solution of complex **1a** (R = ^{i}Pr) with K(HBEt$_3$) afforded the dark red complex [Co{κ^2*N*,*N*′-5-(2,4,6-^{i}Pr$_3$-C$_6$H$_2$)-NC$_4$H$_2$-2-C(H)=N(2,6-^{i}Pr$_2$-C$_6$H$_3$)}(η^6-C$_6$H$_5$CH$_3$)] (**2a**) from a cooled dark red *n*-hexane solution in moderate yields, after workup of the reaction mixture. On the other hand, treating a dark olive-green toluene solution of **1b** (R = Ph) with K(HBEt$_3$), the very dark green complex [Co{κ^2*N*,*N*′-5-[2′-(κ:η^6-C$_6$H$_5$)-C$_6$H$_2$-4′,6′-Ph$_2$]-NC$_4$H$_2$-2-C(H)=N(2,6-^{i}Pr$_2$-C$_6$H$_3$)}] (**2b**) was isolated from

DOI: 10.1021/acs.inorgchem.8b02392
Inorg. Chem. XXXX, XXX, XXX–XXX

a cooled very dark green toluene solution in moderate yields. All reactions with $K(HBEt_3)$ were systematically accompanied by effervescence.

Alternatively, complexes **2a** and **2b** were obtained when the respective precursor complexes **1a** and **1b**, respectively, were reacted with a stoichiometric amount of freshly prepared sodium amalgam in toluene solution, also in moderate yields (Scheme 1, route b).

The pathways for the formation of complexes **2a** and **2b** may be discussed considering their independent synthetic procedures. The synthesis of complexes **2a** and **2b** via reaction of **1a** and **1b** with $K(HBEt_3)$ likely involved the formation of a putative Co(II) hydride bridging dimer complex, $[\{\kappa^2N,N'$-5-(2,4,6-R_3-C_6H_2)-NC_4H_2-2-$C(H)$=N(2,6-^{i}Pr$_2$-C_6H_3)$\}_2Co_2(\mu H,H)]$ (with R = ^{i}Pr or Ph), with formation of KCl and the Py → BEt_3 adduct.[15] This presumed intermediate readily undergoes hydride reductive elimination, with the liberation of molecular dihydrogen (as hinted by the systematic effervescence in these reactions) and subsequent stabilization by coordination of an η^6-arene moiety, either from the reaction solvent, toluene, to form complex **2a**, or via the intramolecular η^6-coordination of one *ortho* phenyl ring present in the 5-(2,4,6-triphenylphenyl) substituent, to form complex **2b**. The synthesis of complexes **2a** and **2b** by the reaction of **1a** and **1b** with sodium amalgam is a one-electron reduction reaction, via the abstraction of the chloride ligand by metallic sodium, with the concomitant inter- or intramolecular substitution of the pyridine ligand by the η^6-arene moiety, respectively.

Complexes **2a** and **2b** are very sensitive to air and moisture, both in the solid state and in solution, despite they may be formally regarded as 18-electron compounds. Complex **2a** is paramagnetic, having a high-spin electronic configuration, with a solution magnetic moment of 3.4 μ_B, in accordance with an $S = 1$ species.[16] Complex **2a** is soluble in *n*-hexane, Et_2O, and toluene, and the lability of the η^6-toluene ligand in **2a** is demonstrated by its easy displacement by C_6D_6 in solutions of this deuterated solvent, with the observation of the complex **2a-C_6D_6** and a free toluene molecule (Scheme 2). The species **2a-C_6D_6**, that is, the species

Scheme 2. Quantitative Displacement of the Toluene Ligand in 2a by C_6D_6 in Benzene-d_6 Solution

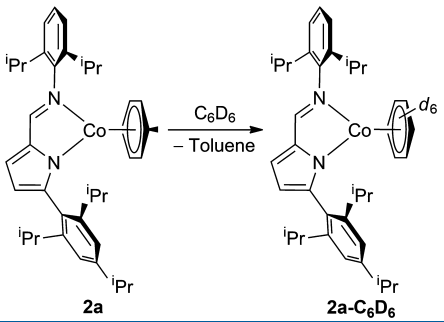

monitored in C_6D_6 solutions of complex **2a**, displays a paramagnetically shifted ^{1}H NMR spectrum with broad resonances accounting for the iminopyrrolyl moiety and a free toluene molecule (Figure S1 of the Supporting Information). In cyclohexane-d_{12}, the ^{1}H NMR spectrum of **2a** shows a similar pattern to that of **2a-C_6D_6** (Figure S2 of the Supporting Information).

However, complex **2b** is partially soluble in *n*-hexane and Et_2O and very soluble in toluene, being diamagnetic at room temperature. Its ^{1}H NMR spectrum in C_6D_6 (Figure S3 of the Supporting Information) shows the expected resonances of the respective 5-(2,4,6-triphenylphenyl)-2-iminopyrrolyl moiety and the absence of free toluene, in contrast with the observations made for complex **2a**. The pyrrolyl protons 3 and 4 appear at 7.64−7.12 and 5.97 ppm, respectively, being slightly shifted to a lower field with respect to the ligand precursor. This same observation is valid for the iminic and the *meta* protons of the central phenyl ring of the 5-(2,4,6-triphenylphenyl) group (7.64−7.12 and 7.97 ppm, respectively). The resonance for the η^6-coordinated phenyl ring *para* proton appears very shifted to a higher field, at 2.00 ppm, in the ^{1}H NMR spectrum, and 104.7 ppm in the $^{13}C\{^1H\}$ NMR spectrum (Figure S4 of the Supporting Information), the cross-peak of which being clearly observed in the $^1H-^{13}C\{^1H\}$ HSQC 2D correlation. This observation is very likely attributed to contact chemical shifts induced by the observed Co(I) complex spin isomerism (see below).

Complexes **2a** and **2b** were characterized by single-crystal X-ray diffraction, having crystallized in the monoclinic system, in the $P2_1/c$ and $P2_1$ space groups, respectively. The structure of complex **2b** has two independent molecules in the asymmetric unit and two cocrystallized toluene molecules. The molecular structures of complexes **2a** and **2b** are presented in Figure 1, and a selection of their bond lengths and angles is presented in Table 1.

Complex **2a** is a Co(I) arene complex with a coordinated toluene molecule through its aromatic system in an η^6-coordination mode, considering that the Co1−Cn (with Cn corresponding to C33 to C38) bond lengths are quite close and fall in the range of 2.150(4)−2.194(3) Å ($\Delta \approx 0.038$ Å). The Co1−centroid distance (with the centroid being defined as the center of the six-membered ring formed by atoms C33 to C38) is equal to 1.6613(16) Å. The Co1−N bond lengths are in the range of 2.025(3)−2.093(3) Å, where the 5-aryl-2-formimino-pyrrolyl ligand exhibits the typical bidentate coordination mode. Both the Co1−N and the Co1−centroid bond lengths are similar to the previously crystalographically characterized Co(I) complexes of the type [LCo(toluene)].[5,6,17] Complex **2a** has a trigonal planar geometry or, considering the tetrahedron formed by the N1, N2, C33, and C36 atoms bonded to Co1, a pseudotetrahedral coordination geometry (with $\tau_4 = 0.74$). The η^6-toluene moiety is perpendicular to the chelation plane (89.11°). The torsions of the 5-aryl and the N2-aryl rings relative to the 2-iminopyrrolyl plane are 80.2(3)° and 83.7(3)°, respectively.

Complex **2b** is also a Co(I) arene complex, resulting from the intramolecular coordination of the *ortho* phenyl ring of the 5-(2,4,6-triphenylphenyl) substituent of the 2-iminopyrrolyl moiety. Complex **2b** contains, therefore, the first case of a 5-aryl-2-iminopyrrolyl with a $\kappa^2N,N'+\kappa C:\eta^6$-coordination mode. The η^6-coordination mode is slightly distorted, as the Co1−Cn (with Cn corresponding to C12 to C17) bond lengths fall in the range of 2.002(9)−2.140(10) Å, with a mean absolute deviation of 0.120 Å for both molecules of the asymmetric unit. The distorted η^6-coordination mode happens at the expense of the rotation of the central ring of 5-(2,4,6-triphenylphenyl) substituent, giving rise to a near-planar π system spanning over the 2-iminopyrrolyl core and the six-membered Co1−N1−C5−C1−C11−C12 chelate. The Co1−centroid distances (with the centroid being defined as the center of the six-membered ring formed by atoms C12 to C17) are in the range of 1.536−1.551 Å. The coordination geometry of complex **2b** can be rationalized as pseudo-square planar, if we consider the plane formed by the N1, N2, C12, and C15 atoms, bonded to Co1 (average $\tau_4 = 0.10$). The Co1−N1 and Co1−N2 bond lengths are in the ranges of 1.847(8)−1.859(7) and 1.883(8)−1.894(7) Å, respectively. The intramolecular arene stabilization observed in **2b** is rare and has

DOI: 10.1021/acs.inorgchem.8b02392
Inorg. Chem. XXXX, XXX, XXX−XXX

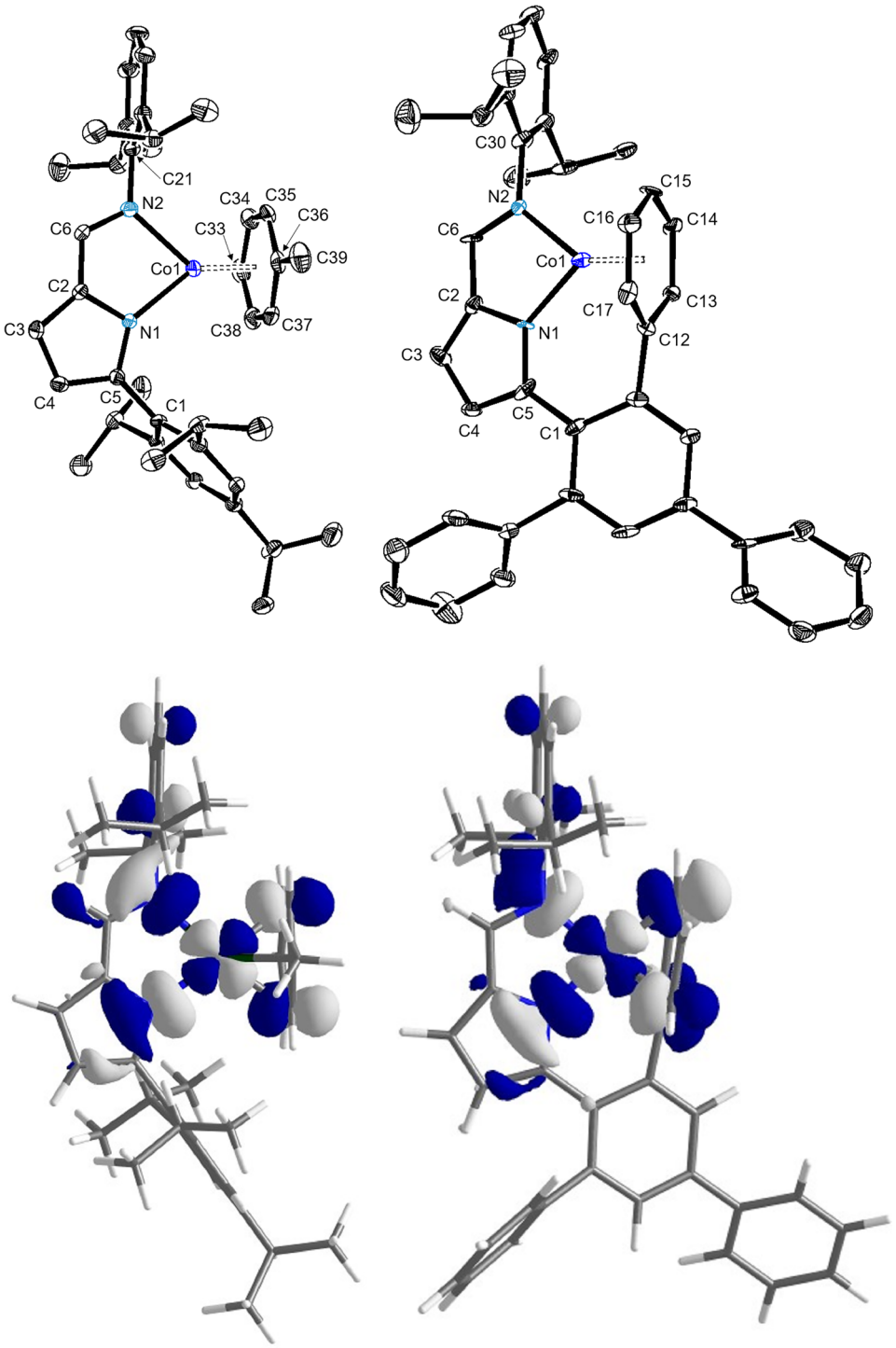

Figure 1. (top) ORTEP-3 diagrams of the X-ray diffraction structures of complexes **2a** (left) and **2b** (right) showing 30% probability ellipsoids. Hydrogen atoms, cocrystallized toluene molecules, and the second molecule in asymmetric unit in the structure of **2b** are omitted for clarity. (bottom) Frontier orbitals of complexes **2a** (left, HOMO) and **2b** (right, LUMO).

been documented in Co complexes bearing the isocyanide C≡NArMes$_2$ (with ArMes$_2$ = 2,6-(2,4,6-Me$_3$C$_6$H$_2$)$_2$-C$_6$H$_3$).[18]

The frontier orbitals of the two species **2a** and **2b** (their frontier orbitals (d-splitting) are presented in Figures S9−S11 of the Supporting Information) confirm the structural discussion above. The LUMO of the closed shell complex (**2b**) can be viewed as the 2b$_{1g}$ orbital of a square planar molecule, based on metal x^2-y^2, and empty in a d^8 species. Conversely, in **2a** the equivalent orbital becomes the single occupied highest occupied molecular orbital (HOMO) of a tetrahedral complex with the same electron count.

On the one hand, considering the superimposition of both 2-iminopyrrolyl Co fragments of **2a** and **2b**, it is very clear that the corresponding η^6-coordinated arenes are staggered, being rotated in relation to each other by ca. 82°. On the other hand, it is critically observed that the bond lengths involving the Co atom of complex **2b** are clearly shorter than those observed for complex **2a** (in average: Δ(Co1−N1) = 0.172 Å, Δ(Co1−N2) = 0.202 Å,

DOI: 10.1021/acs.inorgchem.8b02392
Inorg. Chem. XXXX, XXX, XXX−XXX

Table 1. Selected Bond Lengths (Å) and Angles (deg) for Complexes 2a and 2b

		2b	
	2a	molecule 1	molecule 2
distances (Å)			
Co1−N1	2.025(3)	1.859(7)	1.847(8)
Co1−N2	2.093(3)	1.894(7)	1.883(8)
Co1−C33/C12	2.150(4)	2.022(9)	2.002(9)
Co1−C38/C17	2.154(4)	2.085(9)	2.068(10)
Co1−C37/C13	2.171(4)	2.088(9)	2.092(10)
Co1−C34/C16	2.184(4)	2.114(8)	2.123(10)
Co1−C36/C15	2.188(3)	2.106(9)	2.095(11)
Co1−C35/C14	2.194(3)	2.140(10)	2.110(8)
N1−C5	1.357(4)	1.360(11)	1.372(11)
N1−C2	1.382(4)	1.362(11)	1.388(12)
N2−C6	1.293(4)	1.312(11)	1.313(12)
N2−C_{ipso}	1.433(4)	1.449(11)	1.423(11)
C2−C3	1.386(4)	1.400(12)	1.400(13)
C2−C6	1.403(4)	1.411(12)	1.405(12)
C3−C4	1.383(4)	1.371(13)	1.368(13)
C4−C5	1.404(4)	1.406(12)	1.428(12)
angles (deg)			
N1−Co1−N2	80.56(10)	83.8(3)	84.1(3)
N1−Co1−C33/C12	127.52(12)	89.1(3)	89.6(4)
N2−Co1−C36/C15	123.63(11)	101.8(4)	100.9(4)
C33/C12−Co1−C36/C15	81.39(14)	85.4(4)	85.8(4)
N2−Co1−C33	122.27(14)		
N1−Co1−C36	127.70(12)		
C5−N1−C2	106.4(3)	108.0(8)	110.1(8)
N1−C2−C3	110.0(3)	109.1(8)	107.4(9)
N1−C2−C6	116.7(3)	112.7(9)	112.7(10)
C3−C2−C6	133.2(3)	138.2(10)	139.8(10)
C4−C3−C2	106.9(3)	106.9(8)	107.6(9)
C3−C4−C5	106.9(3)	107.5(8)	108.9(11)
N1−C5−C4	109.9(3)	108.5(8)	105.6(8)
N2−C6−C2	119.5(3)	115.8(9)	115.0(10)

Δ(Co1−N1) = 0.085 Å), attributed to a low-spin electronic state of the former. These two observations reinforce the different electronic structures of **2a** and **2b**.

The Co1−N bond lengths in complexes **2a** and **2b** are shorter than in the family of their Co(II) precursor complexes,[15] highlighting a lower oxidation state (going from a d^7 to a d^8 configuration).

To obtain a toluene-free analogue of complex **2a**, bearing the very reactive "[$Co^{(I)}$\{κ^2*N,N*′-5-(2,4,6-^{i}Pr$_3$-C_6H_2)-NC_4H_2-2-C(H)=N(2,6-^{i}Pr$_2$-C_6H_3)\}]" scaffold, some reactions were attempted in the absence of that solvent. Initially, complex **1a** was reacted with K(HBEt$_3$) in *n*-hexane, from which a color change from dark blue-violet to dark red was observed. After workup, an uncharacterizable mixture of reaction products was observed by ^{1}H NMR spectroscopy. The chemical reduction reactions of complex **1a** in *n*-hexane or Et_2O with sodium amalgam only led to the decomposition of the respective reaction mixtures.

Ultimately, the reaction of complex **1a** with KC_8 in Et_2O afforded the isolation of the dark red binuclear complex [Co\{κ^2*N,N*′-5-(2,4,6-^{i}Pr$_3$-C_6H_2)-NC_4H_2-2-C(H)=N(2,6-^{i}Pr$_2$-C_6H_3)\}]$_2$ (**3**) (Scheme 3, route a). Complex **3** is alternatively prepared by heating complex **2a** in refluxing *n*-hexane (Scheme 3, route b).

The synthesis of complex **3** via reaction of **1a** with KC_8 is a one-electron chemical reduction and shows the preferred stabilization of this system by an arene moiety, as opposed to the coordination of Et_2O. The latter route demonstrated the lability of the toluene ligand of complex **2a** at higher temperatures. The absence of an arene moiety causes the self-assembling of the [Co\{κ^2*N,N*′-5-(2,4,6-^{i}Pr$_3$-C_6H_2)-NC_4H_2-2-C(H)=N(2,6-^{i}Pr$_2$-C_6H_3)\}] synthon into the dimeric complex **3**. As observed for complexes **2a**,**b**, complex **3** is very sensitive to air and moisture and is paramagnetic. In contrast with complex **2a**, which is very soluble in *n*-hexane, complex **3** is only partially soluble in that solvent. The partial solubility of complex **3** in cyclohexane-d_{12} allowed the detection of its ^{1}H NMR spectrum (Figure S5 of the Supporting Information), showing paramagnetically shifted resonances. These facts frustrated the determination of the solution magnetic moment of complex **3** in cyclohexane-d_{12}. The systematic isolation of Co(I) arene complexes strongly suggests that this system is not suitable for the bonding or activation of dinitrogen or weakly coordinating molecules, such as Et_2O. This observation contrasts with the propensity of certain Co complexes bearing *N,N* bidentate anionic ligands for bonding or activating dinitrogen under similar reaction conditions.[4]

Complex **3** crystallized in the triclinic system, in the $P\bar{1}$ space group, and is composed by an asymmetric unit containing the [Co\{κ^2*N,N*′-5-(2,4,6-^{i}Pr$_3$-C_6H_2)-NC_4H_2-2-C(H)=N(2,6-^{i}Pr$_2$-C_6H_3)\}] moiety. Complex **3** is generated by an −*x*, −*y*, −*z* symmetry operation of the previous fragment, with an inversion

Scheme 3. Synthesis of the Dimeric Complex 3[a]

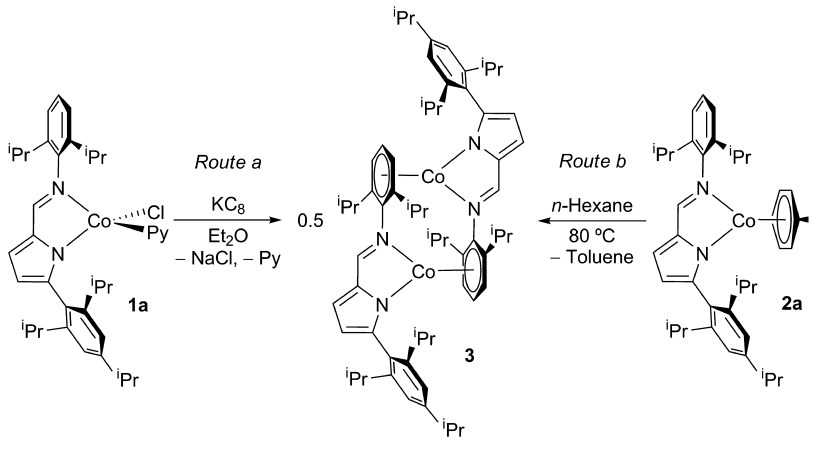

[a]Either by chemical reduction of complex **1a** in Et_2O (route a) or by stirring complex **2a** in refluxing *n*-hexane (route b).

DOI: 10.1021/acs.inorgchem.8b02392
Inorg. Chem. XXXX, XXX, XXX−XXX

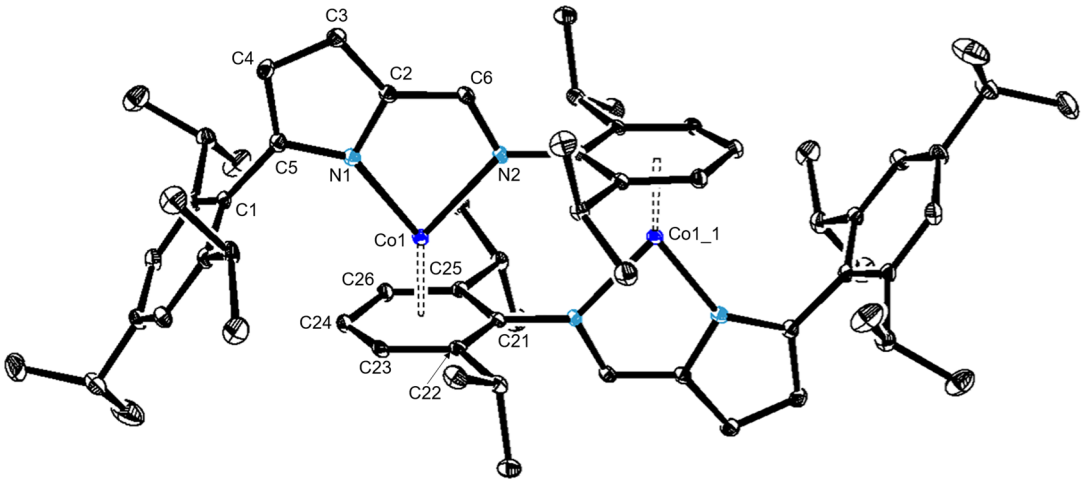

Figure 2. ORTEP-3 diagram of the X-ray diffraction structure of complex **3** showing 30% probability ellipsoids. Hydrogen atoms are omitted for clarity. Selected bond lengths (Å): Co1−N1: 2.020(2), Co1−N2: 2.1691(19), Co1−centroid: 1.6818(9), Co1−C21: 2.183(2), Co1−C22: 2.170(2), Co1−C23: 2.194(2), Co1−C24: 2.260(2), Co1−C25: 2.190(2), Co1−C26: 2.180(2), N1−C5: 1.359(3), N1−C2: 1.373(3), N2−C6: 1.302(3), N2−C21_1: 1.429(3), C1−C5: 1.486(3), C2−C3: 1.403(3), C2−C6: 1.408(3), C3−C4: 1.394(4), C4−C5: 1.405(3). Selected bond angles (deg): N1−Co1−N2: 79.97(8), N1−Co1−C21: 177.25(8), N2−Co1−C21: 97.56(8), N1−Co1−C24: 103.47(9), N2−Co1−C24: 175.57(8), C21−Co1−C24: 79.05(9), C5−N1−C2: 106.13(19), C6−N2−C_{ipso}: 117.0(19), C7−C1−C5: 119.5(2), N1−C2−C3: 110.7(2), N1−C2−C6: 116.7(2), C3−C2−C6: 132.5(2), C4−C3−C2: 105.8(2), C3−C4−C5: 106.8(2), N1−C5−C4: 110.5(2), N1−C5−C1: 120.0(2), C4−C5−C1: 129.5(2), N2−C6−C2: 120.8(2), C20−C18−C19: 109.5(2), C22−C21−C26: 120.8(2), C23−C22−C21: 118.4(2), C24−C23−C22: 122.0(2), C25−C24−C23: 118.6(2), C24−C25−C26: 122.0(2), C25−C26−C21: 118.0(2).

center at [0, 0, 0]. The molecular structure of complex **3** is presented in Figure 2, including selected bond lengths and angles. Complex **3** is a dimer, where the Co atoms are bonded to one 5-aryl-2-iminopyrrolyl ligand in the κ^2N,N' mode and further stabilized by the η^6-coordination of the *N*-2,6-diisopropylphenyl ring of the other unit. The Co1−Cn (with Cn corresponding to C21 to C26) bond lengths are relatively close and fall in the range of 2.170−2.256 Å (Δ ≈ 0.086 Å). The Co1−centroid distance (with the centroid being defined as the center of the six-membered ring formed by carbon atoms C21 to C26) is equal to 1.6818(9) Å. Complex **3** is structurally analogous to complex **2a**, the important variation being the nature of the arene ligand. In the case of complex **3**, the Co1−N1 and Co1−N2 bond lengths are 2.020(2) and 2.1691(19), respectively. This observation contrasts with the very similar Co1−N1 and Co1−N2 bond lengths in complex **2a**. This difference is attributed to the rigidity of the 2,6-diisopropylphenyl ring and the stereochemical stress imparted by the isopropyl groups closer to N2. The torsions of the 5-aryl and the N2-aryl rings relative to the 2-iminopyrrolyl plane are 84.7(3)° and 89.0(2)°, respectively. These results are in accordance with the very few Co(I) complexes of this type.[6,7]

Synthesis and Characterization of a Co(I) Complex Stabilized by Trimethylphosphine. The stabilization of the Co(I) complexes with 5-aryl-2-iminopyrrolyl ligands was also explored with other neutral ligands, such as trimethylphosphine. The salt metathesis reaction of the Co(I) starting material $CoCl(PMe_3)_3$ with the potassium 5-(2,4,6-triisopropylphenyl)-2-(*N*-2,6-diisopropylphenylformimino)pyrrolyl (**KLa**) smoothly afforded the dark red-brown Co(I) complex [Co{κ^2N,N'-5-(2,4,6-^{i}Pr$_3$-C_6H_2)-NC_4H_2-2-C(H)=N(2,6-^{i}Pr$_2$-C_6H_3)}$(PMe_3)_2$] (**4**) in good yields, from a cooled *n*-hexane solution (Scheme 4, route a). Complex **4** can be alternatively prepared by the reaction of $Co(PMe_3)_4$ with the ligand precursor 5-(2,4,6-triisopropylphenyl)-2-(*N*-2,6-diisopropylphenylformimino)-1*H*-pyrrole (**HLa**) (Scheme 4, route b). In this latter case, it is proposed that a NH oxidative addition to the Co(0) center in $Co(PMe_3)_4$ occurs, yielding a putative unobserved Co(II) hydride complex, that readily undergoes reductive elimination, with liberation of molecular dihydrogen, to form complex **4**. This latter observation was similarly reported in the synthesis of bis(trimethylphosphine) bis(2-iminopyrrolyl) Fe complexes by Sun et al.[13h] This latter result reiterates the instability of potential Co(II) hydride complexes to the reaction conditions.

Scheme 4. Synthesis of Complex 4[a]

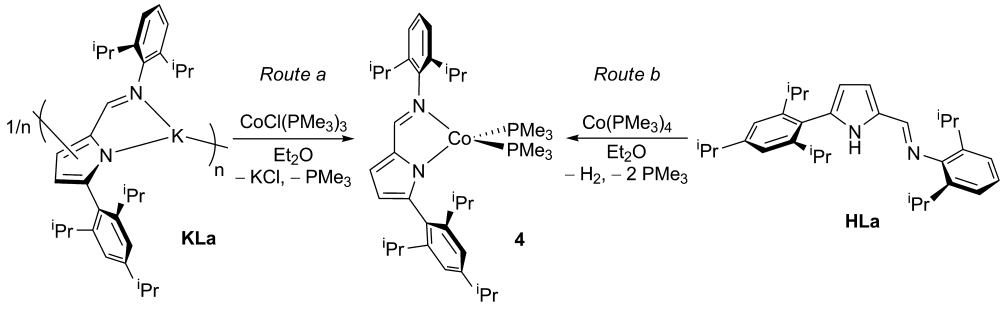

[a]Route a: starting from **KLa** and $CoCl(PMe_3)_3$. Route b: starting from **HLa** and $Co(PMe_3)_4$.

DOI: 10.1021/acs.inorgchem.8b02392
Inorg. Chem. XXXX, XXX, XXX−XXX

Complex **4** is very sensitive to air in solution, but very crystalline samples are relatively stable in the solid state. Complex **4** is formally a 16-electron species, with a solution magnetic moment equal to 3.4 μ_B, which is expected for a d^8 ion in the high-spin state[16] and is in accordance with its paramagnetically shifted and broad ^{1}H NMR spectrum (Figure S6 of the Supporting Information). Despite this paramagnetism, sparse coupling patterns are observed, allowing for partial unambiguous assignments. The PMe_3 proton resonance appears at a very low field, at 69.6 ppm, and displays a broad characteristic, with $\Delta\nu_{1/2}$ equal to 93 Hz. This compound does not display a $^{31}P\{^1H\}$ NMR spectrum.

Complex **4** was characterized by single-crystal X-ray diffraction, having crystallized in the triclinic system, in the $P\bar{1}$ space group. The molecular structure of **4** is presented in Figure 3,

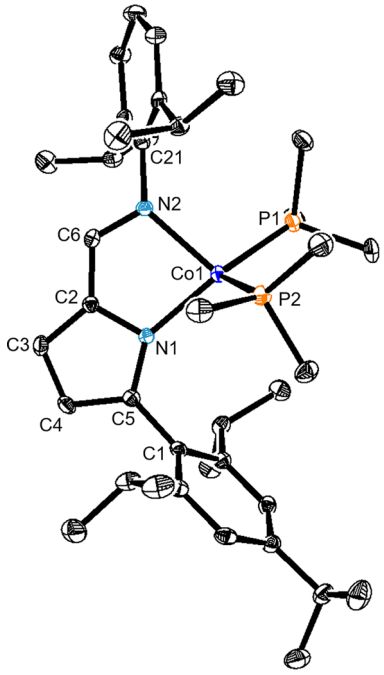

Figure 3. ORTEP-3 diagram of the X-ray diffraction structure of complex **4** showing 30% probability ellipsoids. Hydrogen atoms are omitted for clarity. Selected bond lengths (Å): Co1−N1: 2.026(3), Co1−N2: 2.113(3), Co1−P1: 2.2198(11), Co1−P2: 2.2463(12), N1−C5: 1.365(5), N1−C2: 1.378(5), N2−C6: 1.296(5), N2−C_{ipso}: 1.431(5), C2−C3: 1.387(5), C2−C6: 1.414(5), C3−C4: 1.384(6), C4−C5: 1.399(5), C5−C1: 1.494(5). Selected bond angles (deg): N1−Co1−N2: 82.80(11), N1−Co1−P1: 151.89(9), N2−Co1−P1: 102.18(9), N1−Co1−P2: 99.84(9), N2−Co1−P2: 114.59(9), P1−Co1−P2: 102.94(4), C5−N1−C2: 106.1(3), C6−N2−C_{ipso}: 116.9(3), C3−C2−N1: 110.7(3), C3−C2−C6: 131.4(3), N1−C2−C6: 118.0(3), C2−C3−C4: 106.1(3), C3−C4−C5: 107.6(3), N1−C5−C4: 109.6(3), N1−C5−C1: 123.6(3), C4−C5−C1: 126.7(3), N2−C6−C2: 121.4(3).

including selected bond lengths and angles. Complex **4** is a tetracoordinated complex with a κ^2N,N'-coordinated 5-aryl-2-iminopyrrolyl ligand and two adjacent trimethylphosphine ligands. The Co1−N1 and Co1−N2 bond lengths are 2.026(3) and 2.113(3) Å, respectively, being slightly longer than the ones observed for complex **2a**. This observation is a testament to the higher electronic density in complex **4** due to the higher σ-donating properties of the two trimethylphosphine ligands, giving rise to the largest N1−Co−N2 bite angle of these two monomeric complexes (82.80(11)°). The Co1−P bond lengths are in the range of 2.2198(11)−2.2463(12) Å, which is typical of other crystalographically characterized Co(I) complexes bearing a monoanionic bi- or tridentate chelate and two trimethylphosphine ligands in *cis* positions.[19] Complex **4** has a τ_4 parameter equal to 0.66, which is nearly an intermediate case between a square planar and tetrahedral coordination geometry, probably best described as trigonal pyramidal.

In C_6D_6 solutions, the conversions of complex **2a** into **4** and complex **4** into **2a-C$_6$D$_6$** can be clearly monitored by NMR spectroscopy. In one experiment, treatment of a solid mixture of complex **4** with 1 equiv of 1-azidoadamantane (AdN_3) in C_6D_6 resulted in immediate effervescence of N_2 and formation of complex **2a-C$_6$D$_6$** (Scheme 5), as pointed out by the corresponding

Scheme 5. Chemical Interexchange between Complexes 2a/2a-C$_6$D$_6$ and 4

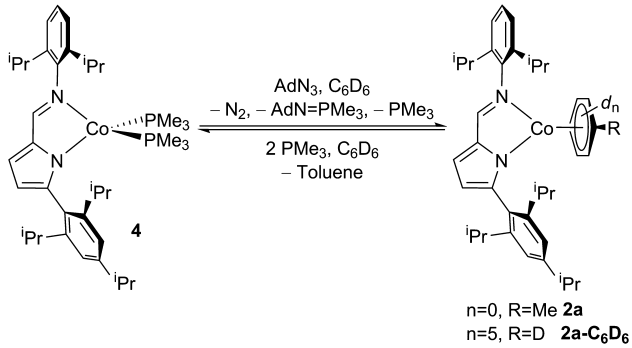

^{1}H NMR spectrum, accompanied by formation of AdN═PMe_3, which is assigned by its $^{31}P\{^1H\}$ NMR spectrum (a singlet at 14.3 ppm−Figure S7 of the Supporting Information).[20] Conversely, complex **2a** is rationally converted to complex **4** by treating the former with 2 equiv of PMe_3 in C_6D_6, as shown by ^{1}H NMR spectroscopy (Scheme 5).

Spin Isomerism in Complex 2b−Experimental Determination of the Energy between Spin Isomers by Variable Temperature NMR Spectroscopy. Spin isomerism in d^4 to d^7 metal complexes has been reported over the years, mainly for Co(III)[21] and for Fe(II) and Fe(III)[22] compounds. More recently, Co(II) complexes have also been reported to exhibit spin isomerism behavior.[23] However, spin isomerism in Co(I) is virtually unknown, except in an example reported by Holland and co-workers of an LCo(CO) complex, with L being a bulky β-diketiminate bidentate ligand identical to that of compound **A** (see Chart 1). In that case, the mechanism for the spin isomerism was a reversible arene slippage stabilization.[24]

The unexpected diamagnetism of complex **2b** prompted us to undergo further studies. First, variable-temperature (VT) ^{1}H NMR experiments were performed and are presented in Figure S8 of the Supporting Information. According to the VT ^{1}H NMR spectra of **2b** it is possible to observe the presence of contact shifts in several resonances as the temperature rises. At 30 °C, the spectrum starts to shift away from the diamagnetic region. As the temperature rises between 30 and 90 °C, some paramagnetic resonances start to appear and become more intense. At 90 °C, complex **2b** displays a paramagnetically shifted ^{1}H NMR spectrum and a loss of resolution, suggesting that an equilibrium between a low-spin (S = 0; singlet, **2b$_{S=0}$**) and high-spin (S = 1; triplet, **2b$_{S=1}$**) isomer is occurring. This effect is reversible, since the spectrum of **2b** at room temperature after cooling is perfectly reproducible.

DOI: 10.1021/acs.inorgchem.8b02392
Inorg. Chem. XXXX, XXX, XXX−XXX

According to this assumption, the chemical shifts of the ^{1}H NMR spectra can be modeled considering a Boltzmann distribution of spin states (details of the model are depicted in the Supporting Information).[21,25,26] The experimental chemical shifts fitted to equation S1 of the Supporting Information as a function of temperature, for three different resonances of complex **2b**, are shown in Figure 4. The thermodynamic data derived from the model for the $\mathbf{2b}_{S=0} \leftrightarrow \mathbf{2b}_{S=1}$ equilibrium is presented in Table 2.

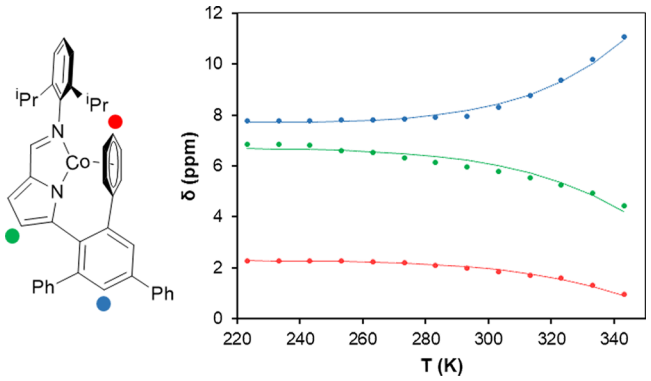

Figure 4. Fittings of the experimental chemical shifts (points), δ (ppm), to the calculated chemical shifts determined by equation S1 of the Supporting Information (solid lines) vs temperature T (K), for different ^{1}H NMR (300 MHz, toluene-d_8) resonances. Blue, green, and red correspond to H8, H4, and H13a protons, respectively, according to the numbering scheme of the Experimental Section.

Table 2. Calculated Values of $\Delta H°$, $\Delta S°$, and $\Delta G°$ (at 298 K) from the Fittings Using Different Resonances and Their Average Values

	Resonances			
Parameter	H8 (blue)	H4 (green)	H13a (red)	Average
$\Delta H°$ (kcal mol^{-1})	8.4	7.3	7.5	7.7
$\Delta S°$ (cal mol^{-1} K^{-1})	9.5	5.9	5.9	7.1
$\Delta G°$ (kcal mol^{-1})	5.5	5.6	5.8	5.6

It can be observed from Figure 4 that the experimental data fit well with the proposed distribution and allowed the calculation of an average positive value of $\Delta G°$ = 5.6 kcal mol^{-1}, at 298 K. This result indicates that this process favors $\mathbf{2b}_{S=0}$, being endothermic ($\Delta H°$ = 7.7 kcal mol^{-1}). The positive value for $\Delta S°$ (7.1 cal mol^{-1} K^{-1}) may be explained by a general increase in the metal-to-ligand bond lengths in the conversion process of $\mathbf{2b}_{S=0}$ into $\mathbf{2b}_{S=1}$ (see below in next subsection).

Spin Isomerism in Complex 2b—DFT Calculations and Determination of the Minimum-Energy Crossing Point. It was experimentally established that complex **2b** exhibits temperature-dependent ^{1}H NMR spectra, being translated in the $\mathbf{2b}_{S=0} \leftrightarrow \mathbf{2b}_{S=1}$ spin equilibrium. We started by examining the structures of both spin isomers by performing the respective geometry optimizations utilizing density functional theory (DFT) calculations, using the OPBE functional. The optimized geometries for both the low-spin ($\mathbf{2b}_{S=0}$) and high-spin ($\mathbf{2b}_{S=1}$) isomers are presented in Figure 5, and the respective atomic coordinates are listed in the Supporting Information.

Looking at the two structures, it can be observed that the Co1—N1 and Co1—N2 bond lengths in $\mathbf{2b}_{S=1}$ are 0.124 and 0.229 Å longer than in $\mathbf{2b}_{S=0}$. Similarly, the Co1—C13a distance in $\mathbf{2b}_{S=1}$ is 0.128 Å longer than that of $\mathbf{2b}_{S=0}$. The observed

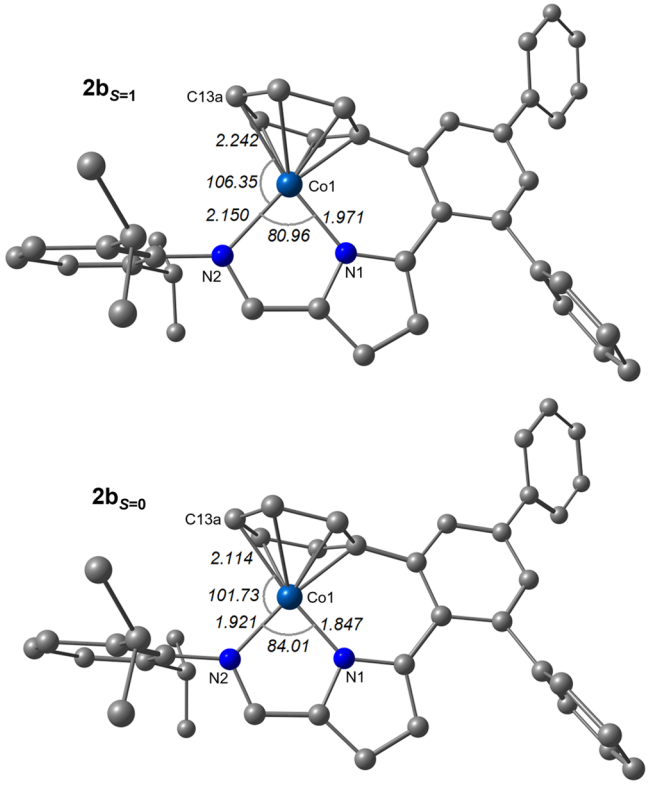

Figure 5. Optimized geometries of the low-spin (bottom, $\mathbf{2b}_{S=0}$) and high-spin (top, $\mathbf{2b}_{S=1}$) isomers, with selected bond lengths (Å) and angles (deg) in italic.

stretch in the bond lengths in $\mathbf{2b}_{S=1}$ is an expected observation for a Co(I) complex in the high-spin state and is achieved at the expense of a slight tilting of the arene ring from orthogonality with the N1—Co1—N2 plane (teapot's or Aladdin lamp's hinged lid type of motion), from 89.98° in $\mathbf{2b}_{S=0}$ to 83.84° in $\mathbf{2b}_{S=1}$. The average increase in the Co1—C_{arene} bond lengths (from $\mathbf{2b}_{S=0}$ to $\mathbf{2b}_{S=1}$) is 0.076 Å, which is lower than the other differences, possibly associated with a slight change of the arene coordination mode in the spin isomers. The frontier orbitals of complex $\mathbf{2b}_{S=1}$ are similar to the ones calculated for **2a**, being typical of a d^8 tetrahedral complex (see Supporting Information). The τ_4 parameters of $\mathbf{2b}_{S=0}$ and $\mathbf{2b}_{S=1}$ increase from 0.13 to 0.19, respectively. This subtle difference indicates a higher tetrahedral distortion of the latter isomer. The experimental bond lengths of complex **2b**, determined by X-ray diffraction, are better reproduced in $\mathbf{2b}_{S=0}$ (maximum absolute variation equal to 0.02 Å). A comparison of experimental and calculated selected structural parameters, for both spin isomers, is presented in Table 3.

Complex $\mathbf{2b}_{S=0}$ is 4.2 kcal mol^{-1} more stable than its high-spin counterpart $\mathbf{2b}_{S=1}$ (ΔE) corroborating the low-spin state observed for the complex and in fair accordance with the experimental stability difference ($\Delta H°$ = 7.7 kcal mol^{-1}).

Analogous calculations were performed for complex **2a**, where the geometries of the spin isomers $\mathbf{2a}_{S=0}$ and $\mathbf{2a}_{S=1}$ were optimized, their respective atomic coordinates being presented in the Supporting Information. In contrast with the spin isomers of **2b**, it was established for **2a** that the high-spin isomer, $\mathbf{2a}_{S=1}$, is 5.6 kcal mol^{-1} below the low-spin one (ΔE), $\mathbf{2a}_{S=0}$. In addition, the experimental bond lengths determined for complex **2a** lie closer to those calculated for the high-spin isomer, $\mathbf{2a}_{S=1}$, with a maximum absolute variation of 0.097 Å (as opposed to a

DOI: 10.1021/acs.inorgchem.8b02392
Inorg. Chem. XXXX, XXX, XXX—XXX

Table 3. Comparison of Selected Structural Parameters of the Single-Crystal X-ray Diffraction Structure of 2b and the Optimized Structures of $2b_{S=0}$ and $2b_{S=1}$

	2b (av exp)	$2b_{S=0}$	$2b_{S=1}$
Co1−N1[a]	1.853(8)	1.847	2.150
Co1−N2[a]	1.888(8)	1.921	1.971
Co1−C13a[a]	2.101(10)	2.114	2.242
N1−Co1−N2[b]	84.0(3)	84.01	80.96
N2−Co1−C13a[b]	101.4(4)	101.73	106.35
τ_4[c]	0.10	0.13	0.19

[a]In angstroms. [b]In degrees. [c]Calculated considering the *square* defined by N1−N2−C13a−C_{ipso} (see Figure 5).

maximum $\Delta(2a-2a_{S=0})$ of 0.166 Å). These observations support the experimental isolation of complexes **2a** and **2b** in two different spin states.

The change in spin state in **2b** from $2b_{S=1}$ to $2b_{S=0}$ corresponds to a spin-forbidden reaction, whereby such a profile goes through a minimum-energy crossing point (MECP) of the two potential energy surfaces (PES) involved, the ones of $2b_{S=0}$ and of $2b_{S=1}$.[27] The structure corresponding to the MECP is $2b_{CP}$. In this MECP, both the energy and the geometry of the molecule are the same in the two surfaces. Once that point is reached along the reaction coordinate, there is a certain probability for the system to change spin state and hop from one PES to the other, giving rise to the "spin-forbidden" reaction.[28] A schematic representation of the spin-state transition alongside the structure of $2b_{CP}$ is presented in Figure 6. The energy of $2b_{CP}$ is 1.6 kcal mol^{-1} above $2b_{S=1}$ indicating a low barrier for the process of spin exchange, in accordance with its experimental observation. The observed low barrier is attributed to the subtle structural changes between the three different structures considered for **2b** (see Table 3).

Hydroboration of Terminal Alkenes and Arylaldehydes Catalyzed by Complexes 2a,b, 3, and 4. With the prepared Co complexes **2a**,**b**, **3**, and **4** being coordinatively unsaturated, in a low oxidation state, and containing two potentially labile ligands in adjacent positions, we decided to test them as catalysts for hydroboration of terminal alkenes and arylaldehydes with pinacolborane (HBPin).

Preliminary hydroboration reactions of styrene with 1% molar of these complexes were attempted, in neat conditions. It was observed that only complex **4** was hydroboration-selective, exclusively yielding the anti-Markovnikov (a-Mk) addition product in 64% yield of isolated product. It should be emphasized that the same reaction performed in the presence of the related catalyst system **1a**/K($HBEt_3$), in similar reaction conditions, led to a much lower yield (35%) and selectivity (a-Mk/Mk = 2.14:1).[15] However, complexes **2a**,**b** and **3** yielded unidentified products. Encouraged by the nearly quantitative selectivity of complex **4**, we tested different terminal alkenes in this reaction. The results for the substrate scope study catalyzed by complex **4** are presented in Table 4, and the ^{1}H NMR spectra of the alkylboronates are shown in Figures S12−S15 of the Supporting Information. As observed with styrene, complex **4** catalyzed the hydroboration of other terminal olefins in high yields and with total selectivity in the anti-Markovnikov addition product.

The yields obtained in this work are in the range of those found by authors reporting cobalt-catalyzed hydroboration of the same alkenes.[10c,d] Even though the presently obtained yields are respectable, some authors have reported yields higher than 90%, for most of the substrates and in less than an hour, in similar reaction conditions.[10b,f,k] The exclusive anti-Markovnikov

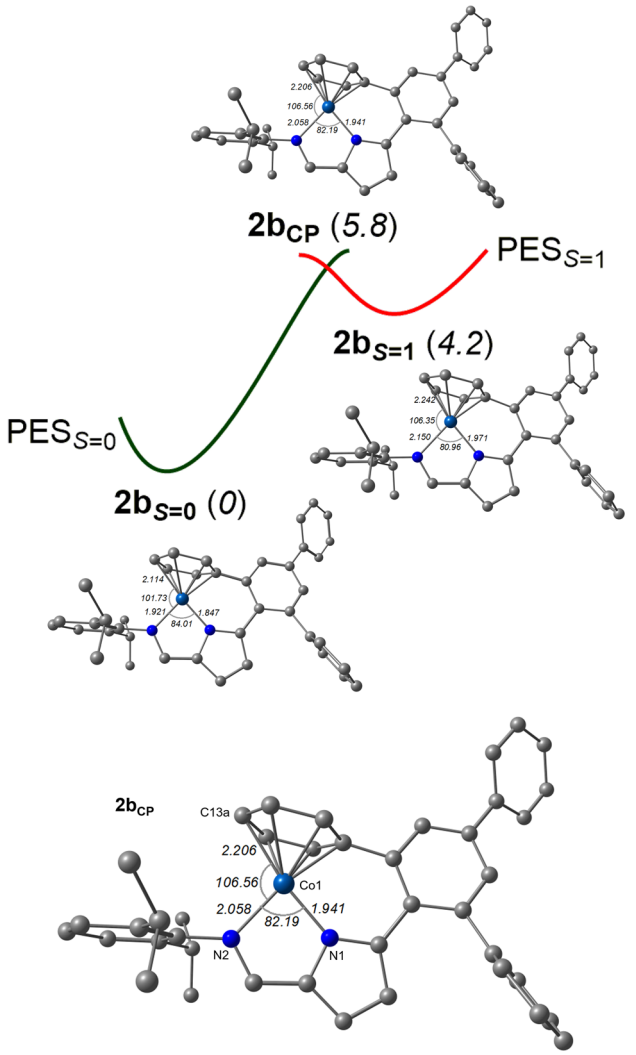

Figure 6. Representation of the MECP of the two PES, with the respective energy balance in italics (in kcal mol^{-1}) (top) and the optimized structure of $2b_{CP}$ (bottom).

selectivity observed in this work follows a common tendency found in the literature surrounding this topic.

All complexes were also tested in the hydroboration of benzaldehyde, in C_6D_6 solutions. The complexes proved to be extremely effective in this reaction, displaying full conversion in less than an hour, with high yields of isolated products. The results of these reactions are presented in Table 5, and the ^{1}H NMR spectra of the obtained boronate esters are shown in the Supporting Information.

Given the high reactivity of these complexes toward the hydroboration of benzaldehyde, the substrate scope of arylaldehydes was evaluated with complex **4**. These results are presented in Table 6, the ^{1}H NMR spectra of the obtained boronate esters being shown in Figures S16−S20 of the Supporting Information. It can be observed that complex **4** is equally effective with other arylaldehydes, also giving rise to fast and complete conversions and high yields in isolated products. In contrast, the hydroboration of acetophenone always gave conversions below 10% after 24 h of reaction. The nearly quantitative yields obtained for this aldehyde scope are in the same range of those reported in the literature for systems containing late transition-metal-based catalytic systems.[11]

Although we have not yet found experimental evidence for the catalytic pathway of these hydroboration reactions, we can propose

DOI: 10.1021/acs.inorgchem.8b02392
Inorg. Chem. XXXX, XXX, XXX−XXX

Table 4. Scope of the Hydroboration of Terminal Alkenes Catalyzed by Complex 4

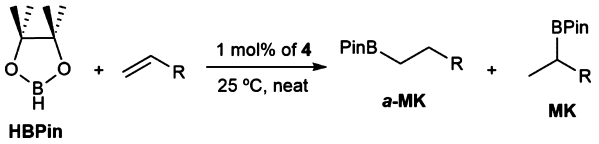

substrate[a]	yield (%)[b]	selectivity (*a*-Mk:Mk)[c]
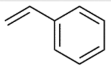	64	>99:1
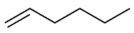	66	>99:1
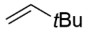	59	>99:1
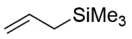	83	>99:1

[a]Conditions: 1 mol % of **4**, 2 mmol of substrate, 2.5 mmol of HBPin. Reaction time: 16 h, temperature: 25 °C. [b]Yields determined by weighing the isolated reaction products. [c]Calculated by ^{1}H NMR.

Table 5. Hydroboration of Benzaldehyde Catalyzed by Complexes 2a,b, 3, and 4 in C_6D_6

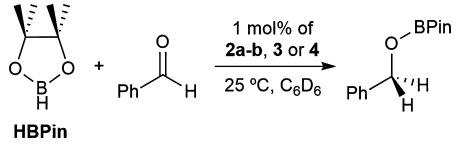

complex[a]	conversion[b] (yield) (%)
2a	>99 (85)
2b	>99 (90)
3	>99 (90)
4	>99 (91)

[a]Conditions: 1 mol % of **2a-b**, **3**, or **4**, 1 mmol of benzaldehyde, 1.1 mmol of HBPin. Reaction time: 1 h, temperature: 25 °C. [b]Conversion calculated by ^{1}H NMR and yields determined by gravimetry weighing the isolated reaction products.

a mechanism whereby there is a partial or full substitution of the Co(I) precatalysts neutral ligands by the organic substrates, which become activated, followed by reaction with HBPin to generate a hypothetic Co(III) intermediate species, possibly via a concerted migratory insertion. A final reductive elimination step, yielding the corresponding organic product and concomitant regeneration of the Co(I) initial species, closes the catalytic cycle (Scheme 6). The improved selectivity in the hydroboration reaction of styrene performed in the presence of complex **4**, when compared to that observed with the catalyst system **1a**/K(HBEt$_3$)[15]—from an a-Mk/Mk ratio of 2.14:1 to greater than 99:1—is justified by the presence of strongly donating PMe_3 ligands, which are not present in the former case. The PMe_3 ligands in complex **4** very likely stabilize the coordination sphere of the intermediate complexes of the respective catalytic cycle, their presence strongly promoting (nearly quantitatively) the formation of terminal addition products.

CONCLUSIONS

Four new Co(I) complexes bearing a 5-aryl-2-iminopyrrolyl ligand and arene or trimethylphosphine ligands have been synthesized, characterized, and tested in the hydroboration of several substrates such as terminal alkenes and arylaldehydes.

Complexes **2a** and **2b** were prepared in moderate yields from the reactions of complexes **1a** and **1b**, respectively, with K(HBEt$_3$) or with Na(Hg) in toluene. Complex **3** was prepared from the reaction of complex **1a** with KC_8 in Et_2O. Finally, complex **4** was prepared in moderate to good yields by salt metathesis of $CoCl(PMe_3)_3$ with the potassium salt **KLa** or by reacting $Co(PMe_3)_4$ with the ligand precursor **HLa**. Complexes **2a**, **3**, and **4** are paramagnetic high-spin species and were characterized by elemental analysis, ^{1}H NMR spectroscopy, and X-ray diffraction.

Table 6. Scope of the Hydroboration of Arylaldehydes Catalyzed by Complex 4 in C_6D_6

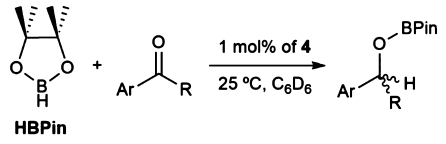

Substrate[a]		Conversion (Yield) (%)[b]
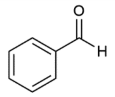	Ar = C_6H_5, R = H	>99 (91)
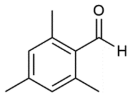	Ar = 2,4,6-Me_3-C_6H_2, R = H	>99 (90)
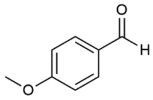	Ar = 4-OMe-C_6H_3, R = H	>99 (95)
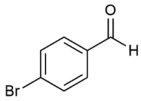	Ar = 4-Br-C_6H_4, R = H	>99 (88)
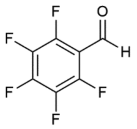	Ar = 2,3,4,5,6-F_5C_6, R = H	>99 (94)
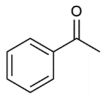	Ar = C_6H_5, R = Me	10[c]

[a]Conditions: 1 mol % of **4**, 1 mmol of benzaldehyde, 1.1 mmol of HBPin. Reaction time: 1 h, temperature: 25 °C. [b]Conversion calculated by ^{1}H NMR and yields determined by weighing the isolated reaction products. [c]Conversion after 24 h.

Scheme 6. Proposed Catalytic Cycle of the Hydroboration of Terminal Alkenes and Arylaldehydes Catalyzed by 2a,b, 3, or 4[a]

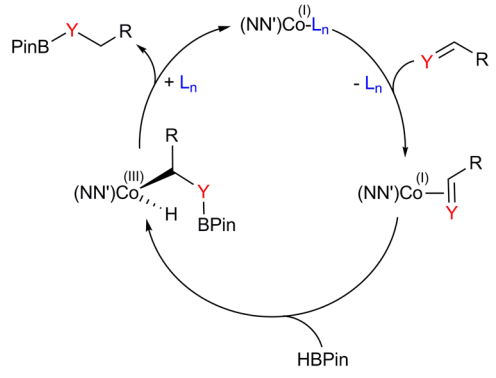

[a]For aldehydes η^1-coordination of the substrate is more favored.[29]

DOI: 10.1021/acs.inorgchem.8b02392
Inorg. Chem. XXXX, XXX, XXX−XXX

However, complex **2b** revealed to be unexpectedly diamagnetic, and it was fully characterized by ^{1}H and ^{13}C{^{1}H} NMR spectroscopy, elemental analysis, and X-ray diffraction. The diamagnetism of **2b** proved to display spin isomerism, as indicated by VT ^{1}H NMR spectroscopy and DFT studies. The VT ^{1}H NMR experiments showed the presence of contact shifts above 30 °C, with $\Delta G°$ (298 K) = 5.6 kcal mol^{-1}, in an endothermic ($\Delta H°$ = 7.7 kcal mol^{-1}) process. Computational studies on complex **2b** showed that the low-spin S = 0 isomer (**2b**$_{S=0}$) is the most stable (ΔE = 4.2 kcal mol^{-1}). The minimum-energy crossing point (**2b**$_{CP}$) was determined, standing 1.6 kcal mol^{-1} above the high-spin isomer (**2b**$_{S=1}$).

All complexes were tested in the hydroboration of styrene, with complex **4** exclusively yielding the respective anti-Markovnikov addition products in high yields. Furthermore, all complexes efficiently catalyzed the hydroboration of benzaldehyde in nearly quantitative yields, in 1 h. Complex **4** was also capable of catalyzing the hydroboration of other terminal alkenes and arylaldehydes in high yields, but the corresponding reaction with acetophenone led to low yields even after 24 h of reaction.

In a complementary perspective, this work provided a good insight of the previously reported reactivity of our pyridine chloride Co(II) complexes **1a**,**b**[15] to form Co(I) species.

EXPERIMENTAL SECTION

General Considerations. All operations were performed under purified dinitrogen atmosphere using standard glovebox and Schlenk techniques unless otherwise stated. Solvents were predried with activated 4 Å molecular sieves and distilled by refluxing under dinitrogen for several hours over suitable drying agents (sodium/benzophenone for diethyl ether and toluene; CaH_2 for *n*-hexane), being stored under dinitrogen. Solvents and solutions were transferred using a positive pressure of dinitrogen through stainless steel cannulae, and mixtures were filtered in a similar way using modified cannulae that could be fitted with glass fiber filter disks. Trimethylphosphine was purchased in 1 M toluene solutions and used as received. K(HBEt$_3$) was purchased in THF solutions and was used as a solid by recrystallization from the same solvent, being stored at 4 °C. Sodium amalgam was prepared inside the glovebox by carefully adding freshly cut sodium metal to mercury with stirring. KC_8 was prepared by mixing freshly cut potassium metal and graphite in the correct stoichiometry inside the glovebox and heating the mixture in a Schlenk tube to 150 °C for 2 h, until a golden solid was observed. The ligand precursor **HLa**,[15] the potassium salt **KLa**,[15] [Co{κ^2*N*,*N*′-5-(2,4,6-^{i}Pr$_3$-C$_6$H$_2$)-NC$_4$H$_2$-2-C(H)═N(2,6-^{i}Pr$_2$-C$_6$H$_3$)}(Py)Cl] (**1a**),[15] [Co{κ^2*N*,*N*′-5-(2,4,6-Ph$_3$-C$_6$H$_2$)-NC$_4$H$_2$-2-C(H)═N(2,6-^{i}Pr$_2$-C$_6$H$_3$)}(Py)Cl] (**1b**),[15] CoCl(PMe$_3$)$_3$,[30] Co(PMe$_3$)$_4$,[30] and 1-azidoadamantane[31] were prepared as described in the literature. All other reagents were acquired commercially and used without further purification.

[Co{κ^2*N*,*N*′-5-(2,4,6-^{i}Pr$_3$-C$_6$H$_2$)-NC$_4$H$_2$-2-C(H)═N(2,6-^{i}Pr$_2$-C$_6$H$_3$)}(η^6-C$_6$H$_5$CH$_3$)] (2a). *Route a.* Toluene was added to a solid mixture of complex **1a** (0.20 g, 0.33 mmol) and K(HBEt$_3$) (0.051 g, 0.36 mmol) at room temperature, to give a dark red solution. The mixture was stirred at room temperature for 2.5 h, to yield a dark red suspension. All volatile materials were evaporated under reduced pressure, to give a dark red residue. The residue was extracted in *n*-hexane with separation of a pale precipitate and a negligible dark residue. The resulting dark red solution was concentrated and stored at −20 °C, giving rise to a dark red crystalline solid suitable for X-ray diffraction. Yield: 0.08 g (42%).

Route b. A toluene solution of complex **1a** (0.25 g, 0.4 mmol) was added to freshly prepared 5% Na(Hg) (0.025 g, 1 mmol of Na; 0.3 mL, 20 mmol of Hg). The dark blue-violet solution gradually turned to a dark red suspension. The mixture was stirred for 4 h at room temperature. The solution was filtered, and the volatile materials were evaporated to dryness to give a dark red residue. The residue was extracted with *n*-hexane, and the extracts were concentrated and stored at −20 °C, to yield a dark red solid. Yield: 0.09 g (37%).

Anal. Calcd for $C_{39}H_{51}CoN_2$, obtained (calculated): C 77.26 (77.20), H 9.59 (8.47), N 4.62 (4.62)%. μ_{eff} (toluene-d_8): 3.4 μ_B. ^{1}H NMR (300 MHz, C$_6$D$_6$): δ 63.03 (s, 1H), 18.67 (br, 1H, C*H*(CH$_3$)$_2$), 17.33 (br, 2H), 13.72 (br, 2H), 10.46 (br, 2H, C*H*(CH$_3$)$_2$), 6.02 (br, 6H, CH(C*H*$_3$)$_2$), 5.26 (br, 6H, CH(C*H*$_3$)$_2$), 4.69 (br, 1H), 3.14 (br, 6H, CH(C*H*$_3$)$_2$), 2.38 (br, 6H, CH(C*H*$_3$)$_2$), 1.94 (br, 6H, CH(C*H*$_3$)$_2$), −4.82 (br, 1H), −37.08 (br, 1H). ^{1}H NMR (300 MHz, cyclohexane-d_{12}): δ 61.87 (s, 1H), 18.61 (br, 1H, C*H*(CH$_3$)$_2$), 17.32 (br, 2H), 13.44 (br, 2H), 9.73 (br, 2H, C*H*(CH$_3$)$_2$), 6.11 (br, 6H, CH(C*H*$_3$)$_2$), 5.28 (br, 6H, CH(C*H*$_3$)$_2$), 4.68 (br, 1H), 3.03 (br, 6H, CH(C*H*$_3$)$_2$), 2.35 (br, 6H, CH(C*H*$_3$)$_2$), 2.02 (br, 6H, CH(C*H*$_3$)$_2$), −4.97 (s, 1H), −36.28 (s, 1H).

[Co{κ^2*N*,*N*′-5-[2′-(κ:η^6-C$_6$H$_5$-C$_6$H$_2$-4′,6′-Ph$_2$)]-NC$_4$H$_2$-2-C(H)═N(2,6-^{i}Pr$_2$-C$_6$H$_3$)}]$_2$ (2b). *Route a.* Toluene was added to a solid mixture of complex **1b** (0.09 g, 0.12 mmol) and K(HBEt$_3$) (0.002 g, 0.14 mmol) at room temperature, to give a very dark green solution. The mixture was stirred at room temperature for 2.5 h, to yield a very dark green suspension. All volatile materials were evaporated under reduced pressure, to give a very dark green residue. The residue was washed with *n*-hexane and extracted with toluene, with separation of a pale precipitate and a negligible dark residue. The very dark green solution was concentrated and stored at −20 °C, giving rise to a very dark green crystalline solid suitable for X-ray diffraction. Yield: 0.08 g (40%).

Route b. A toluene solution of complex **1b** (0.35 g, 0.48 mmol) was added to freshly prepared 5% Na(Hg) (0.025 g, 1 mmol of Na; 0.3 mL, 20 mmol of Hg). The dark olive-green solution gradually turned to a very dark green suspension. The mixture was stirred for 6 h at room temperature. The solution was filtered and the volatile materials were evaporated to dryness to give a very dark green residue. The residue was washed with *n*-hexane, extracted with toluene and the extracts concentrated and stored at −20 °C, yielding a very dark green powder. Yield: 0.10 g (35%).

Anal. Calcd for $C_{41}H_{37}CoN_2$ obtained (calculated): C 79.55 (79.85), H 6.00 (6.05), N 4.42 (4.54)%. ^{1}H NMR (300 MHz, toluene-d_8, 298 K): δ 7.97 (br, 2H, H8a + H12), 7.76 (br, 2H, H8 + H12a), 7.64−7.12 (m, 11H, N = C*H* + H3 + H11 + H13 + H15−17 + H11a), 6.82 (t, 1H, N-Ph-H$_{para}$, $^{3}J_{HH}$ = 6.9 Hz), 5.97 (br, 1H, H4), 3.96 (sept, 2H, C*H*(CH$_3$)$_2$, $^{3}J_{HH}$ = 5.4 Hz), 2.00 (br, 1H, H13a), 1.40 (d, 6H, CH(C*H*$_3$)$_2$, $^{3}J_{HH}$ = 3.0 Hz), 1.03 (d, 6H, CH(C*H*$_3$)$_2$, $^{3}J_{HH}$ = 3.0 Hz). ^{1}H NMR (300 MHz, toluene-d_8, 353 K): δ 12.01, 11.08, 10.32, 9.68, 8.63, 8.22, 6.24, 4.60, 4.25, 1.73, 1.27, 1.10, 0.87, 0.24, −2.18, −2.87, −7.61, −10.11, −12.33, −19.17, −23.72, −32.39, −57.46. ^{1}H NMR (300 MHz, C$_6$D$_6$, 298 K): δ 7.99 (s, 1H, H8a), 7.90 (br, 2H, H12a), 7.81 (s, 1H, H8), 7.79 (s, 1H, N═C*H*), 7.71 (br, 1H, H3), 7.62−7.38 (m, 6H, H11 + H15 + H13 H11a), 7.35−7.19 (m, 5H, H12 + H16 + H17), 7.14−7.06 (m, 2H, N-Ph-H$_{meta}$), 6.88 (t, 1H, N-Ph-H$_{para}$, $^{3}J_{HH}$ = 7.2 Hz), 6.07 (br, 1H, H4), 3.95 (sept, 2H, C*H*(CH$_3$)$_2$, $^{3}J_{HH}$ = 6.6 Hz) 2.00 (br, 1H, H12a), 1.38 (d, 6H, CH(C*H*$_3$)$_2$, $^{3}J_{HH}$ = 4.8 Hz), 1.01 (d, 6H, CH(C*H*$_3$)$_2$, $^{3}J_{HH}$ = 4.5 Hz). ^{13}C{^{1}H} NMR (75 MHz, C$_6$D$_6$, 298 K): δ 151.6 (C10), 145.37 (C14), 144.2 (N-Ph−C$_{ortho}$), 142.4 (C9), 142.6 (C8), 139.9 (C10a), 137.2 (C2 or C5), 136.08 (C2 or C5), 135.1 (C8a), 130.37 (C17), 129.92 (C13), 129.7 (C4), 129.3 (C3), 129.1 (N═CH), 128.99 (C11 + C11a), 127.5 (N-Ph−C$_{para}$), 127.4 (N-Ph−C$_{meta}$), 126.48 (C16), 122.1 (C12 + C12a), 119.2 (C15) 104.7 (C13a), 27.30 (CH(CH$_3$)$_2$), 26.99 (CH(CH$_3$)$_2$), 24.04 (CH(CH$_3$)$_2$), C6, C7 resonances absent.

[Co{κ^2*N*,*N*′-5-(2,4,6-^{i}Pr$_3$-C$_6$H$_2$)-NC$_4$H$_2$-2-C(H)═N(2,6-^{i}Pr$_2$-C$_6$H$_3$)}]$_2$ (3). *Route a.* A solid mixture of complex **1a** (0.40 g, 0.64 mmol) and KC_8 (0.095 g, 0.70 mmol) was suspended in Et$_2$O. The mixture was stirred for 3 h at room temperature, going from a gray-blue to gray-red suspension. The dark red supernatant was filtered, and the volatile materials were evaporated to dryness to give a red solid. The residue was extracted with Et$_2$O, and the extracts were concentrated and stored at −20 °C, to give a red powder. Yield: 0.13 g (40%).

Route b. Complex **2a** (0.35 g, 0.58 mmol) was dissolved in ca. 10 mL of *n*-hexane, and the mixture was stirred for 2 d, at 80 °C. The mixture was stirred while it cooled to room temperature. The dark red supernatant was filtered off at −20 °C, and the red solid was washed with *n*-hexane and dried under vacuum. Yield: 0.20 g (68%).

Anal. Calcd for $C_{64}H_{86}Co_2N_4$, obtained (calculated): C 74.08 (74.68), H 8.56 (8.42), N 5.35 (5.44)%. ^{1}H NMR (300 MHz,

DOI: 10.1021/acs.inorgchem.8b02392
Inorg. Chem. XXXX, XXX, XXX−XXX

cyclohexane-d_{12}): δ 81.06 (br, 2H), 53.07 (br, 2H), 33.67 (br, 2H), 14.66 (br, 12H, CH(CH_3)$_2$), 14.10 (s, 4H, 5-Ph-H$_{meta}$), 12.25 (br, 4H), 10.56 (br, 4H), 7.62 (br, 12H, CH(CH_3)$_2$), 7.02 (br, 12H, CH(CH_3)$_2$), 5.27 (br, 2H), 3.74 (br, 12H, CH(CH_3)$_2$), 2.81 (br, 12H, CH(CH_3)$_2$), 2.27 (br, 2H), −37.28 (br, 2H), −56.19 (br, 2H).

[Co{κ^2*N*,*N*′-5-(2,4,6-^{i}Pr$_3$-C$_6$H$_2$)-NC$_4$H$_2$-2-C(H)═N(2,6-^{i}Pr$_2$-C$_6$H$_3$)}(PMe$_3$)$_2$] (4). *Route a.* An Et$_2$O solution of the potassium ligand salt **KLa** (0.90 mmol, 0.45 g) was added dropwise to a dark blue suspension of CoCl(PMe$_3$)$_3$ (0.90 mmol, 0.29 g) in Et$_2$O, at −80 °C. The mixture was stirred overnight while slowly warming to room temperature. The volatile materials were removed under vacuum to give a dark brown powder. The residue was extracted with *n*-hexane, and the combined extracts were concentrated and stored at −20 °C, yielding a dark red-brown crystalline solid suitable for X-ray diffraction. Yield: 0.37 g (63%).

Route b. An Et$_2$O solution of the ligand precursor **HLa** (0.9 mmol, 0.41 g) was added dropwise to an Et$_2$O solution of Co(PMe$_3$)$_4$ (0.9 mmol, 0.33 g) at −80 °C. The mixture was stirred for 1 h, slowly warming to room temperature, and was further stirred at room temperature for 3 h, to give a dark red-brown solution. The volatile materials were removed under vacuum to give a dark brown residue. The residue was redissolved in *n*-hexane, and the dark red-brown solution was filtered, concentrated, and stored at −20 °C, from which a dark red-brown crystalline solid precipitated. Yield: 0.25 g (42%).

Anal. Calcd for $C_{38}H_{61}CoN_2P_2$, obtained (calculated): C 68.18 (68.45), H 8.71 (9.22), N 4.08 (4.20)%. μ_{eff} (toluene-d_8): 3.4 μ_B. ^{1}H NMR (300 MHz, C_6D_6): δ 73.1 (br, 1H), 69.6 (br, 18H, P(CH_3)$_3$), 68.6 (s, 1H), 36.3 (br, 1H), 5.78 (d, 2H, N-Ph-H$_{meta}$, $^3J_{HH}$ = 6.3 Hz), 3.98 (s, 2H, 5-Ph-H$_{meta}$), 3.80 (br, 6H, CH(CH_3)$_2$), 0.91 (br, 6H, CH(CH_3)$_2$), 0.58 (sept, 1H, CH(CH_3)$_2$, $^3J_{HH}$ = 5.7 Hz), −0.49 (br, 6H, CH(CH_3)$_2$), −1.15 (d, 6H, CH(CH_3)$_2$, $^3J_{HH}$ = 6.3 Hz), −1.40 (br, 6H, CH(CH_3)$_2$), −4.18 (br, 1H), −11.6 (br, 1H), −14.3 (br, 1H), −42.70 (br, 1H).

Generation of 4 from 2a. A dark red C_6D_6 solution of complex **2a** (0.018 g, 0.029 mmol) was treated with PMe$_3$ (0.064 mmol, 0.064 mL of a 1 M solution in toluene), to yield a dark red-brown solution. The ^{1}H NMR spectra was recorded, corresponding to complex **4**.

Generation of 2a-C$_6$D$_6$ from 4. C_6D_6 was carefully added to a solid mixture of complex **4** (0.023 g, 0.035 mmol) and 1-azidoadamantane (0.006 g, 0.035 mmol), giving rise to a dark red solution, with an observable evolution of gas. The ^{1}H NMR spectra was recorded, corresponding to complex **2a-C$_6$D$_6$**, jointly with AdN═PMe$_3$. Data for AdN═PMe$_3$: ^{1}H NMR (300 MHz, C_6D_6): δ 2.24−153 (m, 15H, *Ad*N═P(CH_3)$_3$), 1.00 (br, 9H, AdN═P(CH_3)$_3$). ^{31}P{^{1}H} NMR (121 MHz, C_6D_6): δ 14.3 (AdN═*P*(CH_3)$_3$).

General Procedure for the Hydroboration of Terminal Alkenes Catalyzed by Complex 4. The desired amount of complex (1% mol) was placed in a small Schlenk tube, a solution of the appropriate substrate (2.5 mmol) and pinacolborane (2.75 mmol) was added, and the mixture was stirred for 16 h, at 25 °C. The reaction mixture was quenched by exposing it to air and treating it with *n*-hexane. The solution was filtered through a plug of silica mounted on a Pasteur pipet, and the solvent was evaporated to dryness to yield nearly colorless oils (^{1}H NMR spectra in the Supporting Information). The corresponding yields were determined by weighing the isolated reaction products.

General Procedure for the Hydroboration of Arylaldehydes Catalyzed by Complexes 2a, 2b, 3, and 4. A C_6D_6 solution of the desired amount of complex (1% mol) was added to a solution of the appropriate substrate (1 mmol) and pinacolborane (1.1 mmol), and the mixture was transferred to a J. Young NMR tube. The conversion was measured by ^{1}H NMR after 1 h of reaction (^{1}H NMR spectra in the Supporting Information). The mixture was quenched by exposing it to air and treating it with *n*-hexane. The solution was filtered through a plug of silica mounted on a Pasteur pipet, and the solvent was evaporated to dryness to yield nearly colorless oils. The corresponding yields were determined by weighing the isolated reaction products.

NMR Spectroscopy Measurements. NMR spectra were recorded on a Bruker "AVANCE III" 300 MHz spectrometer at 299.995 MHz (^{1}H), 75.4296 MHz (^{13}C), and 121.439 MHz (^{31}P), referenced internally using the residual protio-resonances (^{1}H) and the solvent carbon (^{13}C) resonances of the corresponding solvents to tetramethysilane (δ = 0) and referenced externally using H_3PO_4 85% (δ = 0) for ^{31}P spectra. Deuterated solvents were dried over activated 4 Å molecular sieves and degassed by the freeze−pump−thaw technique. All samples were prepared inside a glovebox and transferred to J. Young NMR tubes.

Magnetic susceptibility measurements in solution were performed according to the Evans method,[32] using a 3% solution of hexamethyldisiloxane in toluene-d_8. These solutions were prepared in a glovebox in J. Young NMR tubes containing capillary tubes filled with the same solvent mixture, in which the hexamethyldisiloxane is the external reference.

X-ray Crystallography. The crystals were selected under an inert atmosphere, covered with dry and degassed poly(fluoroether) oil (FOMBLIN) and mounted on a nylon loop. Crystallographic data were collected using graphite monochromated Mo Kα radiation (λ = 0.710 73 Å) on a Bruker AXS-KAPPA APEX II diffractometer equipped with an Oxford Cryosystem open-flow nitrogen cryostat, at 150 K. Cell parameters were retrieved using Bruker SMART[33] software and refined using Bruker SAINT[34] on all observed reflections. Absorption corrections were applied using SADABS.[35] Structure solution and refinement were performed using direct methods with the programs SIR2014[36] and SHELXL[37] included in the package of programs WINGX-Version 2014.1.[38] All non-hydrogen atoms were refined anisotropically, and the hydrogen atoms were inserted in idealized positions and allowed to refine riding on the parent carbon atom. Graphic presentations were prepared with ORTEP-3.[39] The crystallographic data for all complexes is presented in Table S1 of the Supporting Information. Data were deposited in CCDC under the deposit numbers 1851719 for **2a**, 1851720 for **2b**, 1851721 for **3**, and 1851722 for **4**. These data are provided free of charge by the Cambridge Crystallographic Data Centre.

Computational Details. All calculations were performed using the Gaussian 09 software package[40] and the OPBE functional. OPBE combines the Handy's OPTX modification of Becke's exchange functional[41] and the gradient-corrected correlation functional of Perdew, Burke, and Ernzerhof.[42] The geometry optimizations were accomplished without symmetry constraints using a standard 6-31G** basis set[43] for all atoms except for cobalt, which used a LanL2DZ basis set[44] with a *f*-polarization function.[45] The MECP (**2b$_{CP}$**) between the spin singlet (S = 0, **2b$_{S=0}$**) and the spin triplet (S = 1, **2b$_{S=1}$**) PES was determined using a code developed by Harvey et al.[46] This code consists of a set of shell scripts and Fortran programs that uses the Gaussian 09 results of energies and gradients of both spin states to produce an effective gradient pointing toward the MECP. Since the MECP is not a stationary point, a standard frequency analysis is not applicable.

■ ASSOCIATED CONTENT

Supporting Information

The Supporting Information is available free of charge on the ACS Publications website at DOI: 10.1021/acs.inorgchem.8b02392.

Characterization data, NMR spectra, crystallographic data, spin isomerism NMR studies, and details of the DFT calculations (PDF)

Accession Codes

CCDC 1851719−1851722 contain the supplementary crystallographic data for this paper. These data can be obtained free of charge via www.ccdc.cam.ac.uk/data_request/cif, or by emailing data_request@ccdc.cam.ac.uk, or by contacting The Cambridge Crystallographic Data Centre, 12 Union Road, Cambridge CB2 1EZ, UK; fax: +44 1223 336033.

■ AUTHOR INFORMATION

Corresponding Author

*E-mail: pedro.t.gomes@tecnico.ulisboa.pt.

ORCID

Tiago F. C. Cruz: 0000-0001-9461-9493

Luís F. Veiros: 0000-0001-5841-3519

Pedro T. Gomes: 0000-0001-8406-8763

DOI: 10.1021/acs.inorgchem.8b02392
Inorg. Chem. XXXX, XXX, XXX−XXX

Notes

The authors declare no competing financial interest.

■ ACKNOWLEDGMENTS

We thank Fundação para a Ciência e a Tecnologia for the financial support (Project No. UID/QUI/00100/2013) and a fellowship to T.F.C.C. and P.T.G. (PD/BD/52372/2013—CATSUS Ph.D. Program and SFRH/BSAB/140115/2018, respectively).

■ REFERENCES

(1) For example: (a) MacKay, B. A.; Fryzuk, M. D. Dinitrogen Coordination Chemistry: On the Biomimetic Borderlands. *Chem. Rev.* **2004**, *104*, 385−401. (b) Fryzuk, M. D.; Johnson, S. A. The continuing story of dinitrogen activation. *Coord. Chem. Rev.* **2000**, *200*−*202*, 379−409.

(2) For example: (a) Gao, K.; Yoshikai, N. Low-Valent Cobalt Catalysis: New Opportunities for C−H Functionalization. *Acc. Chem. Res.* **2014**, *47*, 1208−1219. (b) Yoshida, H. Borylation of Alkynes under Base/Coinage Metal Catalysis: Some Recent Developments. *ACS Catal.* **2016**, *6*, 1799−1811. (c) Bart, S. C.; Hawrelak, E. J.; Lobkovsky, E.; Chirik, P. J. Low-Valent α-Diimine Iron Complexes for Catalytic Olefin Hydrogenation. *Organometallics* **2005**, *24*, 5518−5527.

(3) Camp, C.; Arnold, J. On the non-innocence of "Nacnacs": ligand-based reactivity in β-diketiminate supported coordination compounds. *Dalton Trans.* **2016**, *45*, 14462−14498.

(4) Ding, K.; Pierpont, A. W.; Brennessel, W. W.; Lukat-Rodgers, G.; Rodgers, K. R.; Cundari, T. R.; Bill, E.; Holland, P. L. Cobalt−Dinitrogen Complexes with Weakened N−N Bonds. *J. Am. Chem. Soc.* **2009**, *131*, 9471−9472.

(5) Jones, C.; Schulten, C.; Rose, R. P.; Stasch, A.; Aldridge, S.; Woodul, W. D.; Murray, K. S.; Moubaraki, B.; Brynda, M.; La Macchia, G.; Gagliardi, L. Amidinato− and Guanidinato−Cobalt(I) Complexes: Characterization of Exceptionally Short Co−Co Interactions. *Angew. Chem., Int. Ed.* **2009**, *48*, 7406−7410.

(6) (a) Yang, X.-J.; Fan, X.; Zhao, Y.; Wang, X.; Liu, B.; Su, J.-H.; Dong, Q.; Xu, M.; Wu, B. Synthesis and Characterization of Cobalt Complexes with Radical Anionic α-Diimine Ligands. *Organometallics* **2013**, *32*, 6945−6949. (b) Wang, X.; Zhao, Y.; Gong, S.; Liu, B.; Li, Q.-S.; Su, J.-H.; Wu, B.; Yang, X.-J. Mono- and Dinuclear Heteroleptic Cobalt Complexes with α-Diimine and Polyarene Ligands. *Chem. - Eur. J.* **2015**, *21*, 13302−13310.

(7) Chen, C.; Hecht, M. B.; Kavara, A.; Brennessel, W. W.; Mercado, B. Q.; Weix, D. J.; Holland, P. L. Rapid, Regioconvergent, Solvent-Free Alkene Hydrosilylation with a Cobalt Catalyst. *J. Am. Chem. Soc.* **2015**, *137*, 13244−13247.

(8) Dugan, T. R.; Sun, X.; Rybak-Akimova, E. V.; Olatunji-Ojo, O.; Cundari, T. R.; Holland, P. L. A Masked Two-Coordinate Cobalt(I) Complex That Activates C−F Bonds. *J. Am. Chem. Soc.* **2011**, *133*, 12418−12421.

(9) Pelties, S.; Maier, T.; Herrmann, D.; de Bruin, B.; Rebreyend, C.; Gärtner, S.; Shenderovich, I. G.; Wolf, R. Selective P_4 Activation by a Highly Reduced Cobaltate: Synthesis of Dicobalt Tetraphosphido Complexes. *Chem. - Eur. J.* **2017**, *23*, 6094−6102.

(10) For example: (a) Obligacion, J. V.; Chirik, P. J. Highly Selective Bis(imino)pyridine Iron-Catalyzed Alkene Hydroboration. *Org. Lett.* **2013**, *15*, 2680−2683. (b) Obligacion, J. V.; Chirik, P. J. Bis(imino)-pyridine Cobalt-Catalyzed Alkene Isomerization−Hydroboration: A Strategy for Remote Hydrofunctionalization with Terminal Selectivity. *J. Am. Chem. Soc.* **2013**, *135*, 19107−19110. (c) Palmer, W. N.; Diao, T.; Pappas, I.; Chirik, P. J. High-Activity Cobalt Catalysts for Alkene Hydroboration with Electronically Responsive Terpyridine and α-Diimine Ligands. *ACS Catal.* **2015**, *5*, 622−626. (d) Ibrahim, A. D.; Entsminger, S. W.; Fout, A. R. Insights into a Chemoselective Cobalt Catalyst for the Hydroboration of Alkenes and Nitriles. *ACS Catal.* **2017**, *7*, 3730−3734. (e) Scheuermann, M. L.; Johnson, E. J.; Chirik, P. J. Alkene Isomerization−Hydroboration Promoted by Phosphine-Ligated Cobalt Catalysts. *Org. Lett.* **2015**, *17*, 2716−2719. (f) Ruddy, A. J.; Sydora, O. L.; Small, B. L.; Stradiotto, M.; Turculet, L. (N-Phosphinoamidinate)cobalt-Catalyzed Hydroboration: Alkene Isomerization Affords Terminal Selectivity. *Chem. - Eur. J.* **2014**, *20*, 13918−13922. (g) Zhang, H.; Lu, Z. Dual-Stereocontrol Asymmetric Cobalt-Catalyzed Hydroboration of Sterically Hindered Styrenes. *ACS Catal.* **2016**, *6*, 6596−6600. (h) Zhang, L.; Zuo, Z.; Leng, X.; Huang, Z. A Cobalt-Catalyzed Alkene Hydroboration with Pinacolborane. *Angew. Chem., Int. Ed.* **2014**, *53*, 2696−2700. (i) Peng, J.; Docherty, J. H.; Dominey, A. P.; Thomas, S. P. Cobalt-catalysed Markovnikov selective hydroboration of vinylarenes. *Chem. Commun.* **2017**, *53*, 4726−4729. (j) Zuo, Z.; Yang, J.; Huang, Z. Cobalt-Catalyzed Alkyne Hydrosilylation and Sequential Vinylsilane Hydroboration with Markovnikov Selectivity. *Angew. Chem., Int. Ed. 2017*, *55*, 10839−10843. (k) Zhang, G.; Wu, J.; Wang, M.; Zeng, H.; Cheng, J.; Neary, M. C.; Zheng, S. Cobalt-Catalyzed Regioselective Hydroboration of Terminal Alkenes. *Eur. J. Org. Chem.* **2017**, *2017* (38), 5814−5818. (l) Chen, J.; Xi, T.; Ren, X.; Cheng, B.; Guo, J.; Lu, Z. Asymmetric cobalt catalysts for hydroboration of 1,1-disubstituted alkenes. *Org. Chem. Front.* **2014**, *1*, 1306−1309. (m) Guo, J.; Lu, Z. Highly Chemo-, Regio-, and Stereoselective Cobalt-Catalyzed Markovnikov Hydrosilylation of Alkynes. *Angew. Chem., Int. Ed.* **2016**, *55*, 10835−10838.

(11) For example: (a) Zhang, G.; Zeng, H.; Wu, J.; Yin, Z.; Zheng, S.; Fettinger, J. C. Highly Selective Hydroboration of Alkenes, Ketones and Aldehydes Catalyzed by a Well-Defined Manganese Complex. *Angew. Chem., Int. Ed.* **2016**, *55*, 14369−14372. (b) Tamang, S. R.; Findlater, M. Iron Catalyzed Hydroboration of Aldehydes and Ketones. *J. Org. Chem.* **2017**, *82*, 12857−12862.

(12) Guo, J.; Chen, J.; Lu, Z. Cobalt-catalyzed asymmetric hydroboration of aryl ketones with pinacolborane. *Chem. Commun.* **2015**, *51*, 5725−5727.

(13) (a) Hao, H.; Bhandari, S.; Ding, Y.; et al. Pyrrolylaldiminato Complexes of Zn, Mg and Al. *Eur. J. Inorg. Chem.* **2002**, *2002*, 1060−1065. (b) Panda, T. K.; Yamamoto, K.; Yamamoto, K.; Kaneko, H.; Yang, Y.; Tsurugi, H.; Mashima, K. Preparation and Structure of Iminopyrrolyl and Amidopyrrolyl Complexes of Group 2 Metals. *Organometallics* **2012**, *31*, 2268−2274. (c) Dawson, D. M.; Walker, D. A.; Thornton-Pett, M.; Bochmann, M. Synthesis and reactivity of sterically hindered iminopyrrolato complexes of zirconium, iron, cobalt and nickel. *J. Chem. Soc., Dalton Trans.* **2000**, 459−466. (d) Yoshida, Y.; Matsui, S.; Takagi, Y.; Mitani, M.; Nakano, T.; Tanaka, H.; Kashiwa, N.; Fujita, T. New Titanium Complexes Having Two Pyrrolide−Imine Chelate Ligands: Syntheses, Structures, and Ethylene Polymerization Behavior. *Organometallics* **2001**, *20*, 4793−4799. (e) Mu, J.-S.; Wang, Y.-X.; Li, B.-X.; Li, Y.-S. Synthesis of vanadium(III) complexes bearing iminopyrrolyl ligands and their role as thermal robust ethylene (co)polymerization catalysts. *Dalton Trans.* **2011**, *40*, 3490−3497. (f) Gibson, V. C.; Newton, C.; Redshaw, C.; Solan, G. A.; White, A. J. P.; Williams, D. J. Chromium complexes bearing pyrrolide-imine *N*,*N*-chelate ligands: synthesis, structures and ethylene polymerisation behaviour. *J. Chem. Soc., Dalton Trans.* **2002**, 4017−4023. (g) Li, J.; Song, H.; Cui, C. Synthesis of 2-(*N*-arylimino)pyrrolide nickel complexes and polymerization of methyl methacrylate. *Appl. Organomet. Chem.* **2009**, *24*, 82−85. (h) Jiao, G.; Zhu, G.; Zhang, S.; Sun, H. Synthesis and Characterization of Bis(2-iminopyrrolyl) Iron(II) Complexes by N−H Bond Activation. *Z. Anorg. Allg. Chem.* **2015**, *641* (11), 1959−1963.

(14) (a) Carabineiro, S. A.; Bellabarba, R. M.; Gomes, P. T.; Pascu, S. I.; Veiros, L. F.; Freire, C.; Pereira, L. C. J.; Henriques, R. T.; Oliveira, M. C.; Warren, J. E. Synthesis, Structure and Magnetic Behavior of Five-Coordinate Bis(iminopyrrolyl) Complexes of Cobalt(II) containing PMe_3 and THF Ligands. *Inorg. Chem.* **2008**, *47*, 8896−8911. (b) Carabineiro, S. A.; Silva, L. C.; Gomes, P. T.; Pereira, L. C. J.; Veiros, L. F.; Pascu, S. I.; Duarte, M. T.; Henriques, R. T. Synthesis and Characterization of Tetrahedral and Square Planar Bis(iminopyrrolyl) Complexes of Cobalt(II). *Inorg. Chem.* **2007**, *46*, 6880−6890. (c) Gomes, C. S. B.; Carabineiro, S. A.; Gomes, P. T.; Duarte, M. T.; Lemos, M. A. N. D. A. Octahedral Co(III) complexes of 2-(phenylimino)pyrrolyl ligands: Synthesis and structural characterisation. *Inorg. Chim. Acta* **2011**, *367*, 151−157. (d) Gomes, C. S. B.;

DOI: 10.1021/acs.inorgchem.8b02392
Inorg. Chem. XXXX, XXX, XXX−XXX

Duarte, M. T.; Gomes, P. T. Further iminopyrrolyl complexes of nickel, cobalt, iron and copper: synthesis and structural characterisation. *J. Organomet. Chem.* **2014**, *760*, 167−176. (e) Gomes, C. S. B.; Gomes, P. T.; Duarte, M. T.; Di Paolo, R. E.; Maçanita, A. L.; Calhorda, M. J. Synthesis, Structure, and Photophysical Characterization of Blue-Green Luminescent Zinc Complexes Containing 2-Iminophenanthropyrrolyl Ligands. *Inorg. Chem.* **2009**, *48*, 11176−11186. (f) Cruz, T. F. C.; Figueira, C. A.; Waerenborgh, J. C.; Pereira, L. C. J.; Gomes, P. T.; et al. Synthesis, characterization and magnetism of homoleptic bis(5-aryl-2-iminopyrrolyl) complexes of iron(II) and cobalt(II). *Polyhedron* **2018**, *152*, 179−187.

(15) Cruz, T. F. C.; Lopes, P. S.; Pereira, L. C. J.; Veiros, L. F.; Gomes, P. T. Hydroboration of Terminal Olefins with Pinacolborane Catalyzed by New Mono(2-Iminopyrrolyl) Cobalt(II) Complexes. *Inorg. Chem.* **2018**, *57*, 8146−8159.

(16) (a) Cotton, F. A.; Wilkinson, G.; Murillo, C. A.; Bochmann, M. *Advanced Inorganic Chemistry,* 6th ed.; Wiley, 1999. (b) Greenwood, N. N.; Earnshaw, A. *Chemistry of the Elements,* 2nd ed.; Elsevier Butterworth-Heinemann, 1997.

(17) Dai, X.; Kapoor, P.; Warren, T. H. [Me_2NN]Co(η^6-toluene): O = O, N = N, and O = N Bond Cleavage Provides β-Diketiminato Cobalt μ-Oxo and Imido Complexes. *J. Am. Chem. Soc.* **2004**, *126*, 4798−4799.

(18) (a) Carpenter, A. E.; Margulieux, G. W.; Millard, M. D.; Moore, C. E.; Weidemann, N.; Rheingold, A. L.; Figueroa, J. S. Zwitterionic Stabilization of a Reactive Cobalt Tris-Isocyanide Monoanion by Cation Coordination. *Angew. Chem., Int. Ed.* **2012**, *51*, 9412−9416. (b) Carpenter, A. E.; Rheingold, A. L.; Figueroa, J. S. A Well-Defined Isocyano Analogue of $HCo(CO)_4$. 1: Synthesis, Decomposition, and Catalytic 1,1-Hydrogenation of Isocyanides. *Organometallics* **2016**, *35*, 2309−2318.

(19) For example: (a) Huang, S.; Zhao, H.; Li, X.; Wang, L.; Sun, H. Synthesis of [POCOP]-pincer iron and cobalt complexes via C_{sp3}−H activation and catalytic application of iron hydride in hydrosilylation reactions. *RSC Adv.* **2015**, *5*, 15660−15667. (b) Kent, M. A.; Woodall, C. H.; Haddow, M. F.; McMullin, C. L.; Pringle, P. G.; Wass, D. F. Cobalt PCP Pincer Complexes via an Unexpected Sequence of Ortho Metalations. *Organometallics* **2014**, *33*, 5686−5692. (c) Li, J.; Li, X.; Sun, H. Synthesis and characterization of novel organonickel and organocobalt complexes via carbon−chlorine bond activation. *J. Organomet. Chem.* **2013**, *743*, 114−122. (d) Lian, Z.; Xu, G.; Li, X. [2,6-Bis(diphenylphosphinooxy)phenyl] bis(trimethylphosphine)-cobalt(I). *Acta Crystallogr., Sect. E: Struct. Rep. Online* **2010**, *66*, m636. (e) Xiong, Z.; Li, X.; Zhang, S.; Shi, Y.; Sun, H. Synthesis and Reactivity of N-Heterocyclic PSiP Pincer Iron and Cobalt Complexes and Catalytic Application of Cobalt Hydride in Kumada Coupling Reactions. *Organometallics* **2016**, *35*, 357−363. (f) Xu, G.; Sun, H.; Li, X. Activation of sp^3 Carbon−Hydrogen Bonds by Cobalt and Iron Complexes and Subsequent C−C Bond Formation. *Organometallics* **2009**, *28*, 6090−6095. (g) Zhao, H.; Li, X.; Zhang, S.; Sun, H. Synthesis and Characterization of Iron, Cobalt, and Nickel [PNP] Pincer Amido Complexes by N−H Activation. *Z. Anorg. Allg. Chem.* **2015**, *641*, 2435−2439. (h) Zhu, G.; Li, X.; Xu, G.; Wang, L.; Sun, H. A new PC(sp^3)P ligand and its coordination chemistry with low-valent iron, cobalt and nickel complexes. *Dalton Trans.* **2014**, *43*, 8595−8598. (i) Zhu, G.; Wang, L.; Sun, H.; Li, X. Formation of PCP pincer cobalt complexes with cobaltacyclopropane moieties via double Csp^3−H bond activation. *RSC Adv.* **2015**, *5*, 19402−19408.

(20) Kogut, E.; Wiencko, H. L.; Zhang, L.; Cordeau, D. E.; Warren, T. H. A Terminal Ni(III)−Imide with Diverse Reactivity Pathways. *J. Am. Chem. Soc.* **2005**, *127*, 11248−11249.

(21) (a) Gütlich, P.; McGarvey, B. R.; Kläui. Temperature-dependent $^5T_2(O_h) \leftrightarrow {}^1A_1(O_h)$ spin equilibrium in a six-coordinate cobalt(III) complex. Investigation by ^{31}P NMR in solution. *Inorg. Chem.* **1980**, *19*, 3704−3706. (b) Kläui, W.; Eberspach, W.; Gütlich, P. Spin-crossover cobalt(III) complexes: steric and electronic control of spin state. *Inorg. Chem.* **1987**, *26*, 3977−3982.

(22) Gütlich, P.; Goodwin, H. A. Spin Crossover—An Overall Perspective. *Top. Curr. Chem.* **2004**, *234*, 23−47.

(23) Krivokapic, I.; Zerara, M.; Daku, M. L.; Vargas, A.; Enachescu, C.; Ambrus, C.; Tregenna-Piggott, P.; Amstutz, N.; Krausz, E.; Hauser, A. Spin-crossover in cobalt(II) imine complexes. *Coord. Chem. Rev.* **2007**, *251*, 364−378.

(24) Al-Afyouni, M. H.; Suturina, E.; Pathak, S.; Atanasov, M.; Bill, E.; DeRosha, D. E.; Brennessel, W. W.; Neese, F.; Holland, P. L. Spin Isomers and Ligand Isomerization in a Three-Coordinate Cobalt(I) Carbonyl Complex. *J. Am. Chem. Soc.* **2015**, *137*, 10689−10699.

(25) (a) Eaton, D. R.; Phillips, W. D.; Caldwell, D. J. Configurations and Magnetic Properties of the Nickel(II) Aminotroponeimineates. *J. Am. Chem. Soc.* **1963**, *85*, 397−406. (b) Eaton, D. R.; Phillips, W. D. Nuclear Magnetic Resonance of Paramagnetic Molecules. *Adv. Magn. Opt. Reson.* **1965**, *1*, 103−148. (c) Pignolet, L. H.; Horrocks, W. D. Direct observation of the rate of planar-tetrahedral equilibrium of four-coordinate nickel(II) by nuclear magnetic resonance. Diastereoisomeric Dihalobis(dissymmetric tertiary phosphine)nickel(II) complexes. *J. Am. Chem. Soc.* **1969**, *91*, 3976−3978.

(26) Smith, M. E.; Andersen, R. A. Me_5C_5Ni(acac): A Monomeric, Paramagnetic, 18-Electron, Spin-Equilibrium Molecule. *J. Am. Chem. Soc.* **1996**, *118*, 11119−11128.

(27) For reviews on MECP and their location for transition-metal complexes, see: (a) Harvey, J. N.; Poli, R.; Smith, K. M. Understanding the reactivity of transition metal complexes involving multiple spin states. *Coord. Chem. Rev.* **2003**, *238*−*239*, 347−361. (b) Poli, R.; Harvey, J. N. Spin forbidden chemical reactions of transition metal compounds. New ideas and new computational challenges. *Chem. Soc. Rev.* **2003**, *32*, −8.1

(28) Harvey, J. N. Understanding the kinetics of spin-forbidden chemical reactions. *Phys. Chem. Chem. Phys.* **2007**, *9*, 331−343.

(29) For M = Fe: (a) Gorgas, N.; Stöger, B.; Veiros, L. F.; Pittenauer, E.; Allmaier, G.; Kirchner, K. Efficient Hydrogenation of Ketones and Aldehydes Catalyzed by Well-Defined Iron(II) PNP Pincer Complexes: Evidence for an Insertion Mechanism. *Organometallics* **2014**, *33*, 6905−6914. For M = Mn: (b) Gorgas, N.; Stöger, B.; Veiros, L. F.; Kirchner, K. Highly Efficient and Selective Hydrogenation of Aldehydes: A Well-Defined Fe(II) Catalyst Exhibits Noble-Metal Activity. *ACS Catal.* **2016**, *6*, 2664−2672.

(30) Klein, H.-F.; Karsch, H. H. Methyltetrakis(trimethy1phosphin)-kobalt und seine Derivate. *Chem. Ber.* **1975**, *108*, 944−955.

(31) Sasaki, T.; Eguchi, S.; Katada, T.; Hiroaki, O. Synthesis of adamantane derivatives. 37. A convenient and efficient synthesis of 1-azidoadamantane and related bridgehead azides, and some of their reactions. *J. Org. Chem.* **1977**, *42*, 3741−3743.

(32) (a) Evans, D. F. 400. The determination of the paramagnetic susceptibility of substances in solution by nuclear magnetic resonance. *J. Chem. Soc.* **1959**, 2003−2005. (b) Sur, S. K. Measurement of magnetic susceptibility and magnetic moment of paramagnetic molecules in solution by high-field fourier transform NMR spectroscopy. *J. Magn. Reson.* **1989**, *82*, 169−173.

(33) *SMART,* Software for the CCD Detector System Version 5.625; Bruker AXS Inc.: Madison, WI, 2001.

(34) *SAINT,* Software for the CCD Detector System, Version 7.03; Bruker AXS Inc.: Madison, WI, 2004.

(35) Sheldrick, G. M. *SADABS,* Program for Empirical Absorption Correction; University of Göttingen: Göttingen, Germany, 1996.

(36) Burla, M. C.; Caliandro, R.; Carrozzini, B.; Cascarano, G. L.; Cuocci, C.; Giacovazzo, C.; Mallamo, M.; Mazzone, A.; Polidori, G. Crystal structure determination and refinement via SIR2014. *J. Appl. Crystallogr.* **2015**, *48*, 306.

(37) (a) Sheldrick, G. M. Crystal structure refinement with SHELXL. *Acta Crystallogr., Sect. C: Struct. Chem.* **2015**, *71*, 3−8. (b) Hübschle, C. B.; Sheldrick, G. M.; Dittrich, B. *ShelXle*: a Qt graphical user interface for SHELXL. *J. Appl. Crystallogr.* **2011**, *44*, 1281−1284.

(38) (a) Farrugia, L. J. WinGX suite for small-molecule single-crystal crystallography. *J. Appl. Crystallogr.* **1999**, *32*, 837−838. (b) Farrugia, L. J. *J. Appl. Crystallogr.* **2012**, *45*, 849−854.

(39) (a) Burnett, M. N.; Johnson, C. K. *ORTEP-III: Oak Ridge Thermal Ellipsoid Plot Program for Crystal Structure Illustration;* Oak Ridge National Laboratory, 1996. Report ORNL-6895. (b) Farrugia, L.

DOI: 10.1021/acs.inorgchem.8b02392
Inorg. Chem. XXXX, XXX, XXX−XXX

J. ORTEP-3 for Windows − a version of ORTEP-III with a Graphical User Interface (GUI). *J. Appl. Crystallogr.* **1997**, *30*, 565.

(40) Frisch, M. J.; Trucks, G. W.; Schlegel, H. B.; Scuseria, G. E.; Robb, M. A.; Cheeseman, J. R.; Scalmani, G.; Barone, V.; Mennucci, B.; Petersson, G. A.; Nakatsuji, H.; Caricato, M.; Li, X.; Hratchian, H. P.; Izmaylov, A. F.; Bloino, J.; Zheng, G.; Sonnenberg, J. L.; Hada, M.; Ehara, M.; Toyota, K.; Fukuda, R.; Hasegawa, J.; Ishida, M.; Nakajima, T.; Honda, Y.; Kitao, O.; Nakai, H.; Vreven, T.; Montgomery, J. A., Jr.; Peralta, J. E.; Ogliaro, F.; Bearpark, M.; Heyd, J. J.; Brothers, E.; Kudin, K. N.; Staroverov, V. N.; Kobayashi, R.; Normand, J.; Raghavachari, K.; Rendell, A.; Burant, J. C.; Iyengar, S. S.; Tomasi, J.; Cossi, M.; Rega, N.; Millam, J. M.; Klene, M.; Knox, J. E.; Cross, J. B.; Bakken, V.; Adamo, C.; Jaramillo, J.; Gomperts, R.; Stratmann, R. E.; Yazyev, O.; Austin, A. J.; Cammi, R.; Pomelli, C.; Ochterski, J. W.; Martin, R. L.; Morokuma, K.; Zakrzewski, V. G.; Voth, G. A.; Salvador, P.; Dannenberg, J. J.; Dapprich, S.; Daniels, A. D.; Farkas, Ö.; Foresman, J. B.; Ortiz, J. V.; Cioslowski, J.; Fox, D. J. *Gaussian 09,* Revision A.01; Gaussian, Inc.: Wallingford, CT, 2009.

(41) (a) Handy, N. C.; Cohen, A. J. Left-right correlation energy. *Mol. Phys.* **2001**, *99*, 403−412. (b) Hoe, H.-M.; Cohen, A.; Handy, N. C. Assessment of a new local exchange functional OPTX. *Chem. Phys. Lett.* **2001**, *341*, 319−328.

(42) (a) Perdew, J. P.; Burke, K.; Ernzerhof, M. Generalized Gradient Approximation Made Simple. *Phys. Rev. Lett.* **1996**, *77*, 3865−3868. (b) Perdew, J. P.; Burke, K.; Ernzerhof, M. Generalized Gradient Approximation Made Simple. *Phys. Rev. Lett.* **1997**, *78*, 1396.

(43) (a) McLean, A. D.; Chandler, G. S. Contracted Gaussian basis sets for molecular calculations. I. Second row atoms, Z = 11−18. *J. Chem. Phys.* **1980**, *72*, 5639−5648. (b) Krishnan, R.; Binkley, J. S.; Seeger, R.; Pople, J. A. Self-consistent molecular orbital methods. XX. A basis set for correlated wave functions. *J. Chem. Phys.* **1980**, *72*, 650−654. (c) Wachters, A. J. H. Gaussian Basis Set for Molecular Wavefunctions Containing Third-Row Atoms. *J. Chem. Phys.* **1970**, *52*, 1033. (d) Hay, P. J. Gaussian basis sets for molecular calculations. The representation of 3d orbitals in transition-metal atoms. *J. Chem. Phys.* **1977**, *66*, 4377−4384. (e) Raghavachari, K.; Trucks, G. W. Highly correlated systems. Excitation energies of first row transition metals Sc−Cu. *J. Chem. Phys.* **1989**, *91*, 1062−1089. (f) Curtiss, L. A.; et al. Extension of Gaussian-2 theory to molecules containing third-row atoms Ga−Kr. *J. Chem. Phys.* **1995**, *103*, 6104. (g) McGrath, M. P.; Radom, L. Extension of Gaussian-1 (G1) theory to bromine containing Molecules. *J. Chem. Phys.* **1991**, *94*, 511−516.

(44) (a) Dunning, T. H., Jr.; Hay, P. J. *Modern Theoretical Chemistry;* Schaefer, H. F., III, Ed.; Plenum: New York, 1976; Vol. *3*, p 1. (b) Hay, P. J.; Wadt, W. R. Ab initio effective core potentials for molecular calculations. Potentials for the transition metal atoms Sc to Hg. *J. Chem. Phys.* **1985**, *82*, 270. (c) Wadt, W. R.; Hay, P. J. Ab initio effective core potentials for molecular calculations. Potentials for main group elements Na to Bi. *J. Chem. Phys.* **1985**, *82*, 284. (d) Hay, P. J.; Wadt, W. R. Ab initio effective core potentials for molecular calculations. Potentials for K to Au including the outermost core orbitals. *J. Chem. Phys.* **1985**, *82*, 299.

(45) Ehlers, A. W.; Böhme, M.; Dapprich, S.; Gobbi, A.; Höllwarth, A.; Jonas, V.; Köhler, K. F.; Stegmann, R.; Veldkamp, A.; Frenking, G. A set of f-polarization functions for pseudo-potential basis sets of the transition metals Sc−Cu, Y−Ag and La−Au. *Chem. Phys. Lett.* **1993**, *208*, 111.

(46) Harvey, J. N.; Aschi, M.; Schwarz, H.; Koch, W. The singlet and triplet states of phenyl cation. A hybrid approach for locating minimum energy crossing points between non-interacting potential energy surfaces. *Theor. Chem. Acc.* **1998**, *99*, 95−99.

DOI: 10.1021/acs.inorgchem.8b02392
Inorg. Chem. XXXX, XXX, XXX−XXX